Recent developments and challenges for (Q)RPA-based methods

7-9 July 2026

From QRPA to Finite-Temperature QRPA: Formalism and Applications

Esra Yüksel

School of Mathematics and Physics,

University of Surrey, Guildford, Surrey, United Kingdom

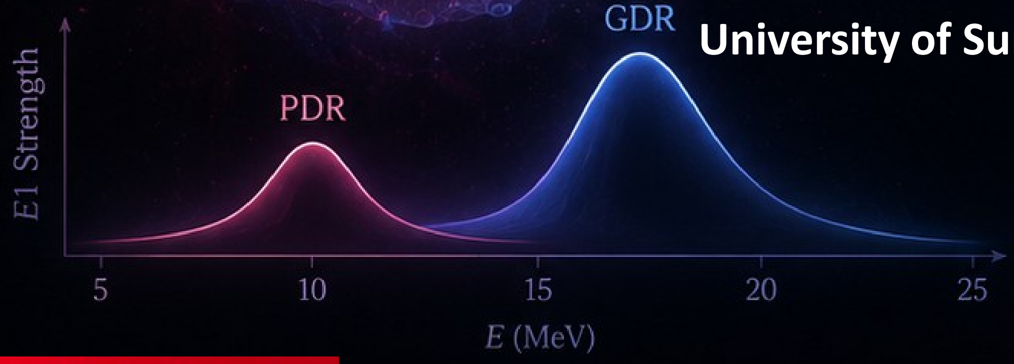

DE LA RECHERCHE À L'INDUSTRIE

cea

ESNT

Espace de Structure Nucléaire Théorique

DSM - DAM

UNIVERSITY OF SURREY

Outline

1. Motivation: why finite-temperature response?
2. Thermodynamic starting point
3. Deriving FT-RPA
4. Why FT-RPA is not enough: pairing
5. Deriving FT-QRPA
6. Limits of FT-RPA and FT-QRPA

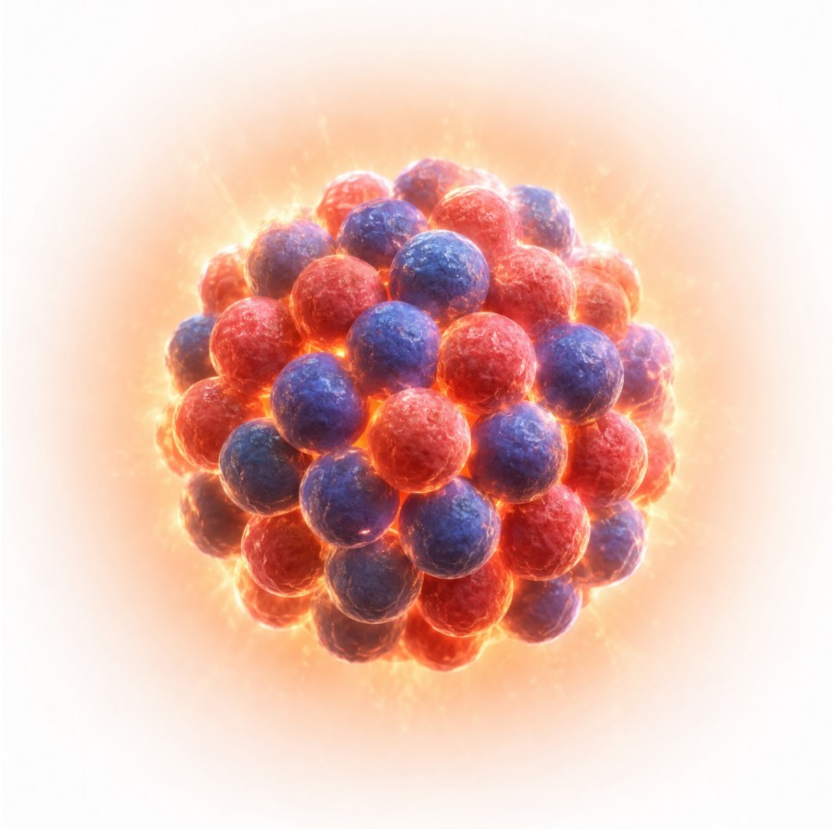

Motivation: why finite-temperature response?

Giant Resonances

	Isoscalar	Isovector	
Monopole GMR	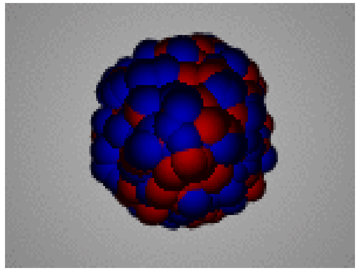	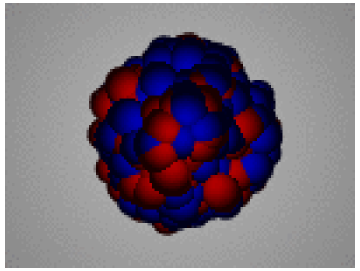	
Dipole GDR		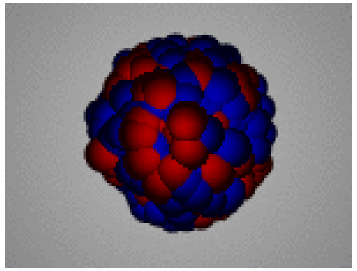	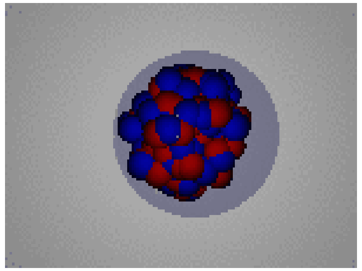
Quadrupole GQR	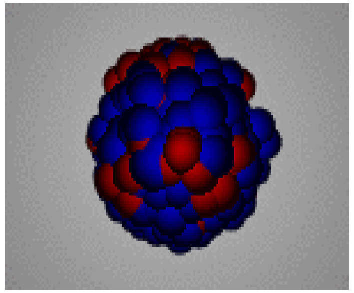	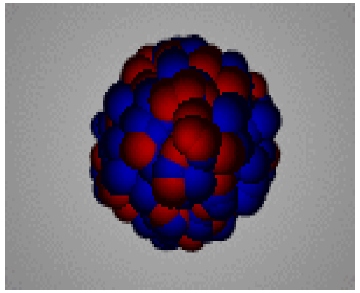	

Schematic representation of giant resonances.
Ref: Kernphysik Homepage(H.J.Wollersheim) (gsi.de)

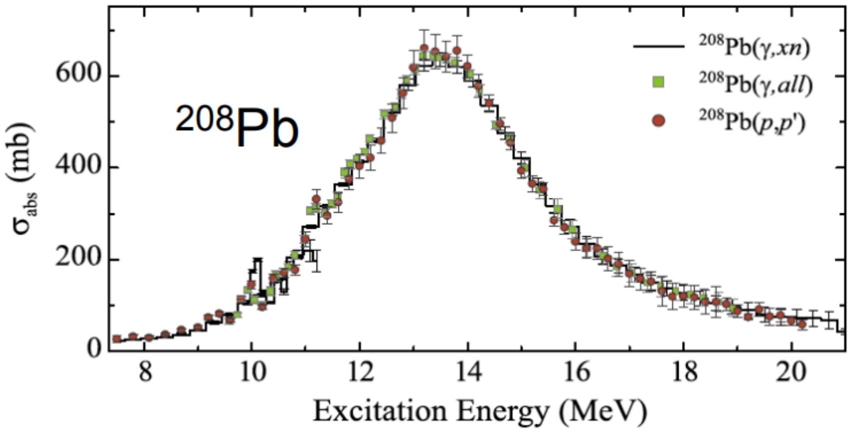

A. Tamii, P. von Neumann-Cosel, I. Poltoratska, EPJ A 50 (2), 28 (2014)

- ✓ **GRs carry information about the fundamental properties of nuclei**
- ✓ GRs are crucial in nuclear astrophysics for understanding key processes such as nucleosynthesis in stars and supernovae.
- ✓ GRs provide direct constraints on nuclear incompressibility, symmetry energy, effective mass, and surface properties.

Motivation: Giant Resonances at finite temperature

- ✓ Giant resonances contribute to γ-ray strength functions, which influence nuclear reaction rates.

- ✓ In stellar and explosive astrophysical environments, finite-temperature E1 γ-strength functions affect radiative-capture and photodisintegration rates, thereby impacting nucleosynthesis.

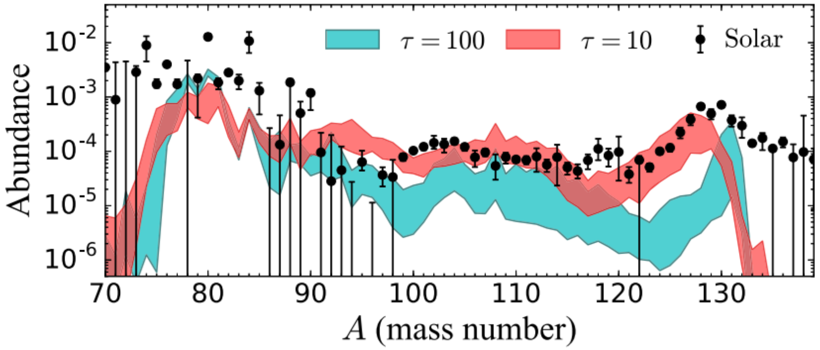

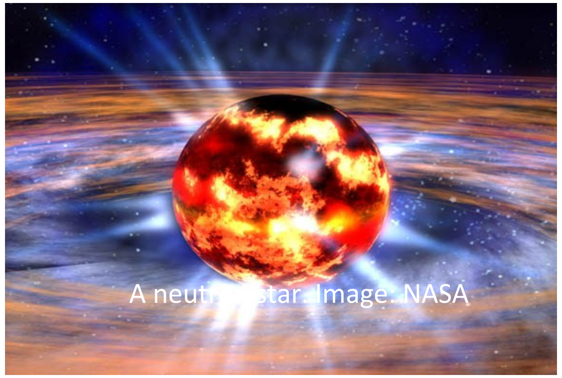

The Astrophysical Journal, 855:99 (9pp), 2018

- ✓ How do nuclear excitations evolve with increasing temperature?

- ✓ Self-consistent mean-field theories (HF(B), Q(RPA)) are standing as the prominent tools for calculations.

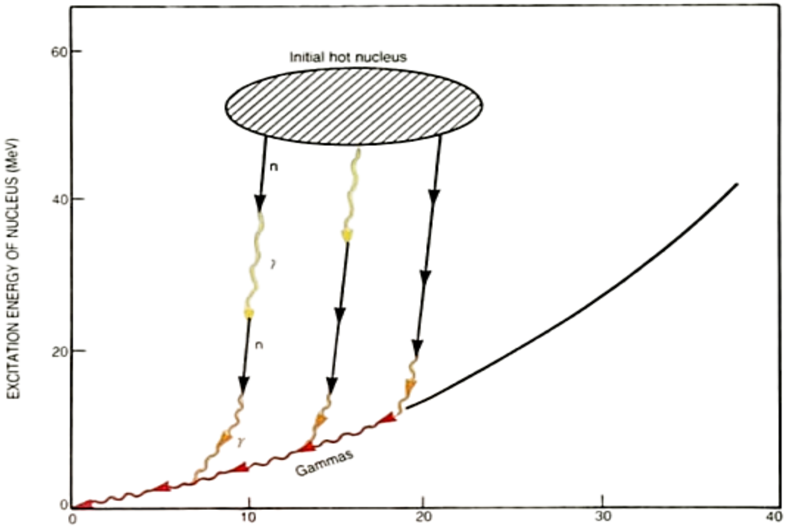

Giant Resonances in Hot Nuclei, George F. Bertsch; Ricardo A. Broglia

- ✓ The hot IVGDR is the main experimentally accessible giant resonance in highly excited nuclei.

- ✓ Experimental studies are mainly based on high-energy γ decay from hot compound nuclei populated in **heavy-ion fusion–evaporation reactions.**

Motivation: Hot pygmy dipole strength? (HOT-PDS)

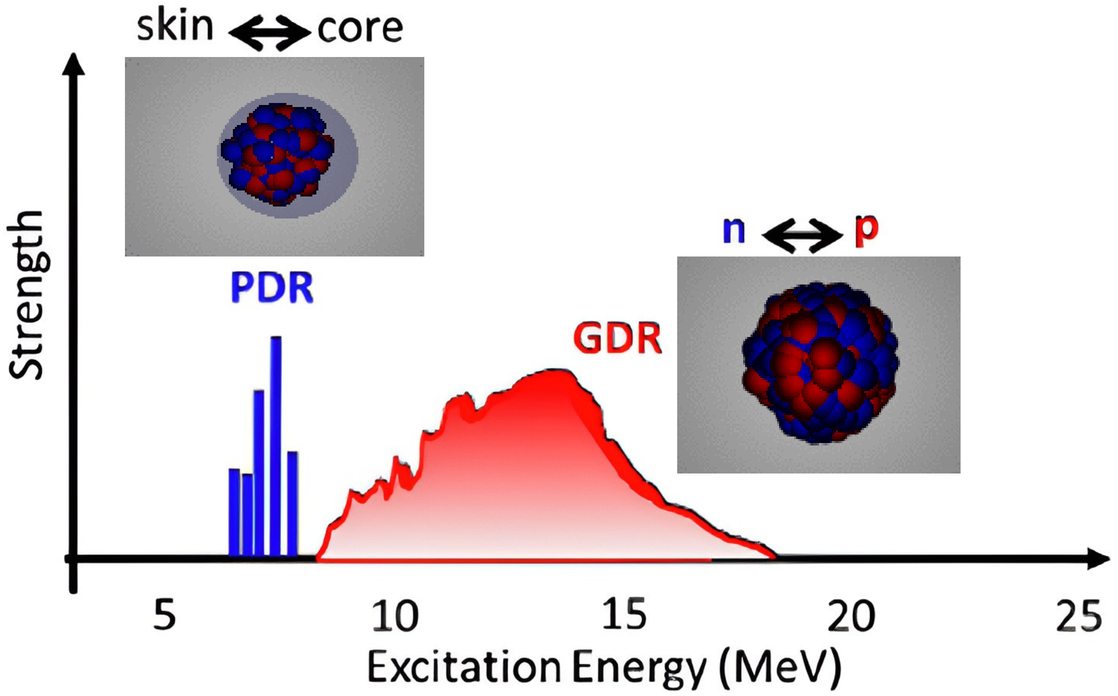

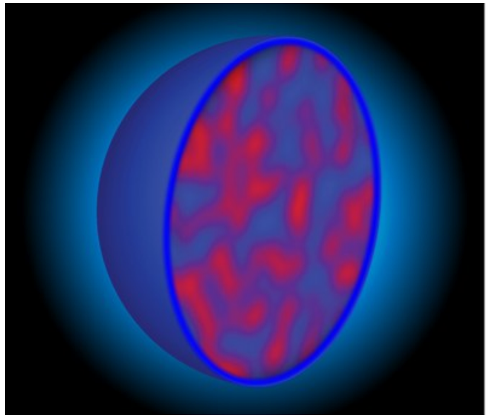

Neutron skin thickness

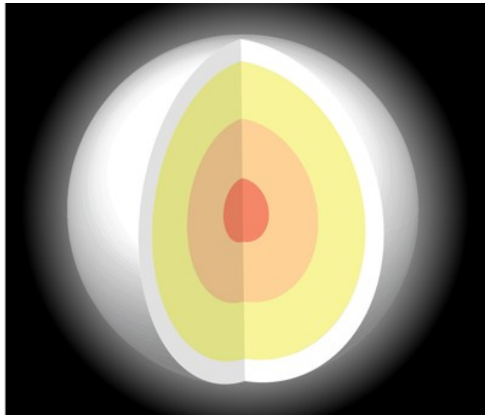

EOS → Neutron star

Credit for figure: https://physics.aps.org/articles/v14/58

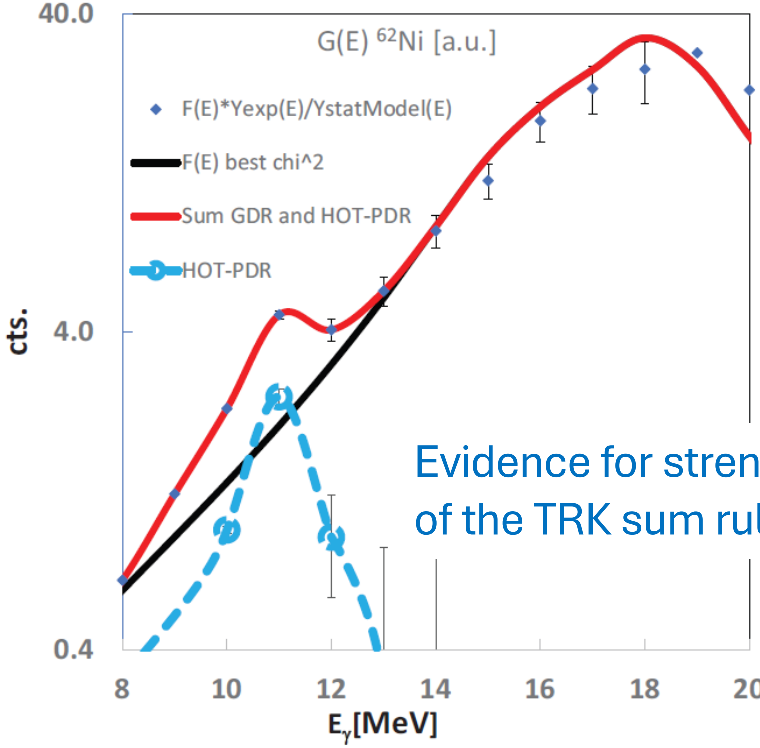

O. Wieland et.al., IL NUOVO CIMENTO 47 C (2024) 24

Evidence for strength up to ≈ 4% of the TRK sum rule in hot 62Ni

- IFIN 9MV Tandem facility in Romania: They study γ decay from hot, thermalized compound nuclei: ^{56}Ni*, ^{60}Ni*, ^{62}Ni $\langle T \rangle \approx$ **1.6 MeV**
- For ^{60}Ni and ^{62}Ni : A clear excess yield appears below the GDR centroid, around 10 MeV.
- **Hot PDS? Microscopic studies are needed!**

Motivation: weak interaction processes at finite temperature

- *Spin–isospin response plays a central role in stellar weak-interaction processes.*

- ***β −decay rates of neutron-rich nuclei*** *governs r-process timescales and abundance patterns, with contributions from Gamow–Teller and first-forbidden transitions.*

- **Electron capture** shapes the electron fraction and collapse dynamics

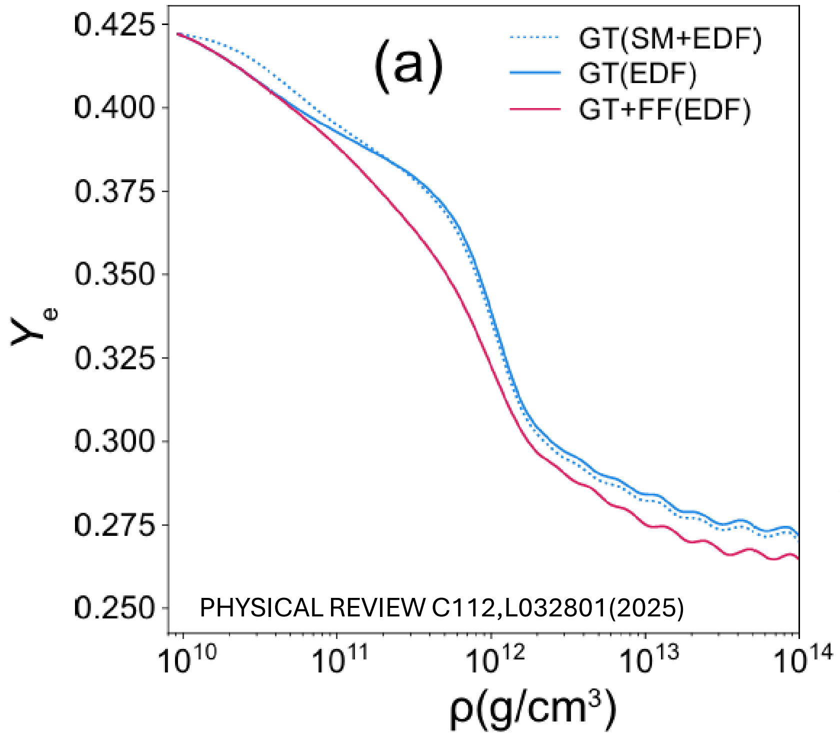

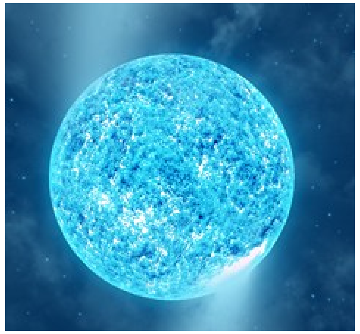

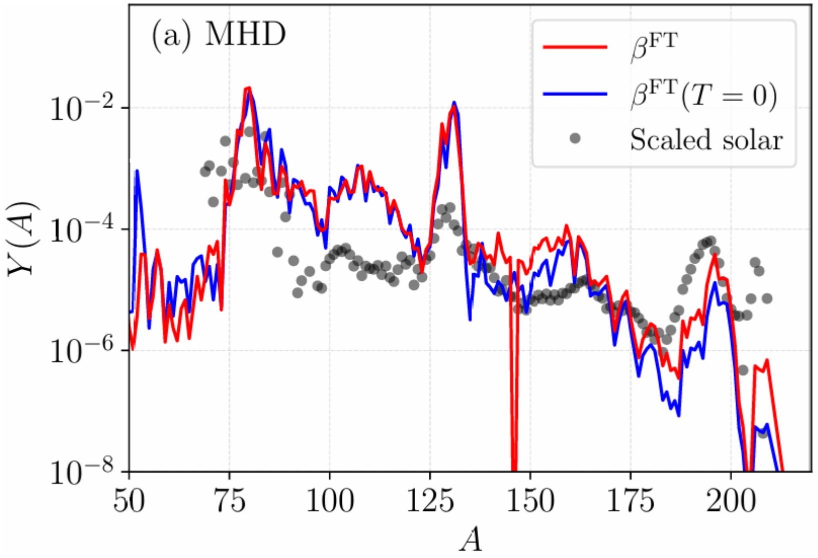

The Astrophysical Journal,1001:85(12pp),2026April10

In stellar matter, weak rates depend on temperature, density, and nuclear excitations.

Finite-temperature HFB/BCS + charge-exchange QRPA provide a microscopic framework for these calculations.

Finite temperature HF-RPA

Nuclei at finite temperature can be treated as open systems that exchange both heat and particles described within the grand-canonical ensemble. Such a system is characterized by its grand-potential:

$$\Omega[\rho] = E[\rho] - TS[\rho] - \lambda_n N[\rho] - \lambda_p Z[\rho],$$

By minimizing the Grand canonical potential $\delta\Omega = 0,$

$$f_i(T) = \frac{1}{1+\exp[(\varepsilon_i - \lambda_\tau)/k_B T]}, \qquad \tau = n, p.$$

$$\rho(\mathbf{r}, T) = \sum_{i\tau} f_{i\tau}(T)|\phi_{i\tau}(\mathbf{r})|^2.$$

$$\boxed{f_i(T) \xrightarrow[T\to 0]{} \begin{cases} 1, & \varepsilon_i < \lambda_\tau, \\ 0, & \varepsilon_i > \lambda_\tau, \end{cases} \qquad \rho(\mathbf{r}, T) \to \sum_{h \in \text{occ.}} |\phi_h(\mathbf{r})|^2.}$$

We use $k_B = 1$, so T is expressed in MeV.

a) Single-particle energies around fermi level

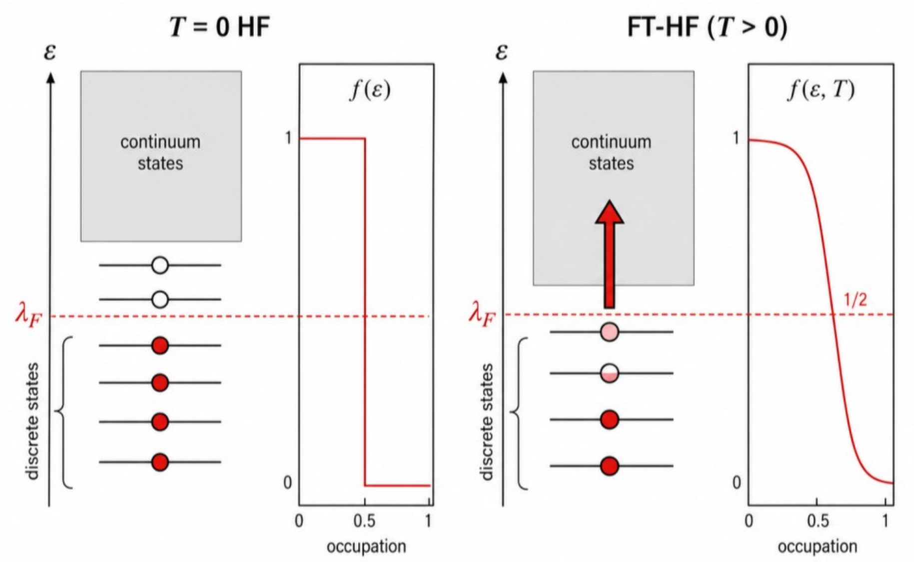

b) Density profile

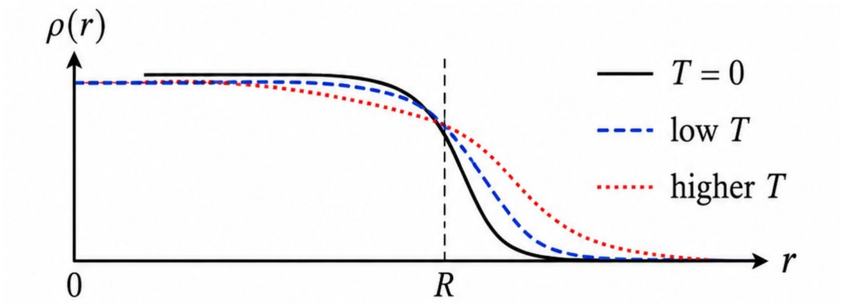

Finite temperature HF-RPA: impact on configuration space

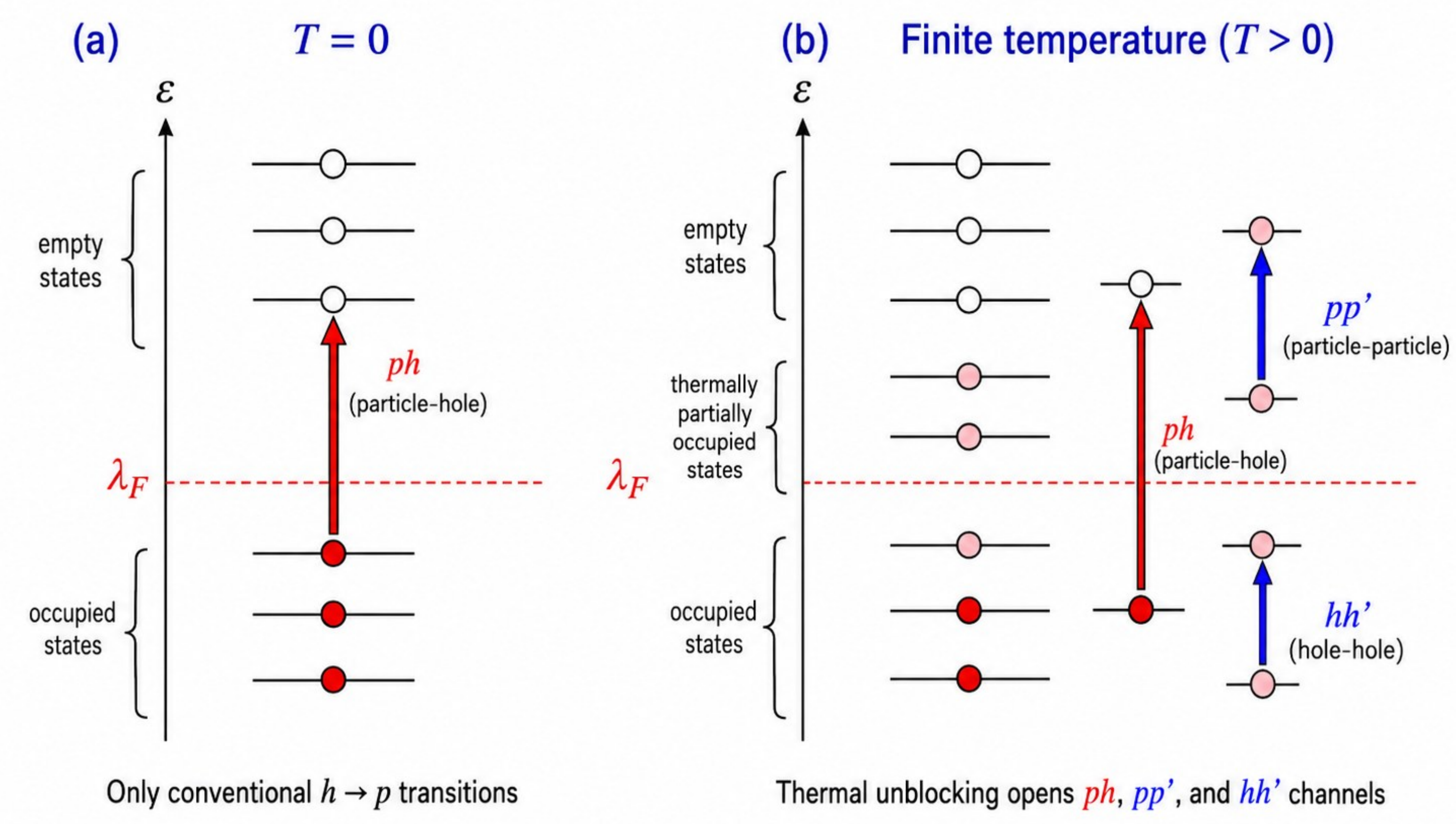

Derivation of finite temperature HF-RPA

Thermal Hartree-Fock basis

$$h_0|i\rangle = \varepsilon_i|i\rangle, \qquad \rho^0_{ij} = \langle c^\dagger_j c_i\rangle_T = \delta_{ij} f_i,$$

For an ordered thermally allowed transition,

$$\varepsilon_i < \varepsilon_m, \qquad f_i > f_m.$$

$$C^\dagger_{mi} = c^\dagger_m c_i, \qquad C_{mi} = c^\dagger_i c_m = (C^\dagger_{mi})^\dagger.$$

thermal commutator norm of a particle–hole operator.

$$\begin{aligned}\langle [C_{mi}, C^\dagger_{m'i'}]\rangle_T &= \delta_{mm'}\langle c^\dagger_i c_{i'}\rangle_T - \delta_{ii'}\langle c^\dagger_{m'} c_m\rangle_T \\ &= \delta_{mm'}\delta_{ii'} f_i - \delta_{ii'}\delta_{mm'} f_m \\ &= \boxed{\boxed{(f_i - f_m)}\delta_{mm'}\delta_{ii'}}.\end{aligned}$$

At finite temperature, each transition has a different norm. The available phase space is $f_i - f_m$. At zero temperature, for a hole-to-particle transition, this factor becomes $f_h - f_p = 1$, so ordinary RPA is recovered.

Standard RPA excitation operator

$$Q^\dagger_\nu = \sum_{mi}\left(X^\nu_{mi} C^\dagger_{mi} - Y^\nu_{mi} C_{mi}\right),$$

For a neutral excitation, the transition operators conserve particle number, so the projected equation of motion can be written with the physical many-body Hamiltonian

$$\left\langle [C_{mi}, [\hat{H}, Q^\dagger_\nu]]\right\rangle_T = E_\nu \left\langle [C_{mi}, Q^\dagger_\nu]\right\rangle_T, \qquad E_\nu = \hbar\omega_\nu.$$

$$= E_\nu (f_i - f_m) X^\nu_{mi}.$$

***LHS**: Double-commutator matrices*

$$\mathcal{A}_{mi,m'i'} \equiv \left\langle [C_{mi}, [\hat{H}, C^\dagger_{m'i'}]]\right\rangle_T,$$

$$\mathcal{B}_{mi,m'i'} \equiv -\left\langle [C_{mi}, [\hat{H}, C_{m'i'}]]\right\rangle_T.$$

Projected equation of motion: A, B, and the FT-RPA matrix

The forward projected equation is

$$\sum_{m'i'} \left(\mathcal{A}_{mi,m'i'} X^{\nu}_{m'i'} + \mathcal{B}_{mi,m'i'} Y^{\nu}_{m'i'} \right) = E_{\nu} (f_i - f_m) X^{\nu}_{mi}.$$

Thermal Wick factorization gives

$$\mathcal{A}_{mi,m'i'} = (f_i - f_m) \left[(\varepsilon_m - \varepsilon_i) \delta_{mm'} \delta_{ii'} + (f_{i'} - f_{m'}) V^{\text{res}}_{mi,i'm'} \right],$$

$$\mathcal{B}_{mi,m'i'} = (f_i - f_m)(f_{i'} - f_{m'}) V^{\text{res}}_{mi,m'i'}.$$

The simplified forward FT-RPA equation is then

$$\hbar\omega_{\nu} X^{\nu}_{mi} = \sum_{m'i'} \left[A^{(w)}_{mi,m'i'} X^{\nu}_{m'i'} + B^{(w)}_{mi,m'i'} Y^{\nu}_{m'i'} \right],$$

$$A^{(w)}_{mi,m'i'} = (\varepsilon_m - \varepsilon_i) \delta_{mm'} \delta_{ii'} + \boxed{(f_{i'} - f_{m'})} V^{\text{res}}_{mi,i'm'},$$

$$B^{(w)}_{mi,m'i'} = \boxed{(f_{i'} - f_{m'})} V^{\text{res}}_{mi,m'i'}.$$

Projected equation of motion: A, B, and the FT-RPA matrix

For a Hermitian residual kernel, define

$$\tilde{X}^{\nu}_{mi} = \sqrt{(f_i - f_m)}\, X^{\nu}_{mi}, \qquad \tilde{Y}^{\nu}_{mi} = \sqrt{(f_i - f_m)}\, Y^{\nu}_{mi}.$$

$$\boxed{\begin{pmatrix} \tilde{A} & \tilde{B} \\ -\tilde{B}^* & -\tilde{A}^* \end{pmatrix} \begin{pmatrix} \tilde{X}^{\nu} \\ \tilde{Y}^{\nu} \end{pmatrix} = \hbar\omega_{\nu} \begin{pmatrix} \tilde{X}^{\nu} \\ \tilde{Y}^{\nu} \end{pmatrix}.}$$

$$\tilde{A}_{mi,m'i'} = (\varepsilon_m - \varepsilon_i)\delta_{mm'}\delta_{ii'} + \sqrt{(f_i - f_m)(f_{i'} - f_{m'})}\, V^{\mathrm{res}}_{mi,i'm'},$$

$$\tilde{B}_{mi,m'i'} = \sqrt{(f_i - f_m)(f_{i'} - f_{m'})}\, V^{\mathrm{res}}_{mi,m'i'}.$$

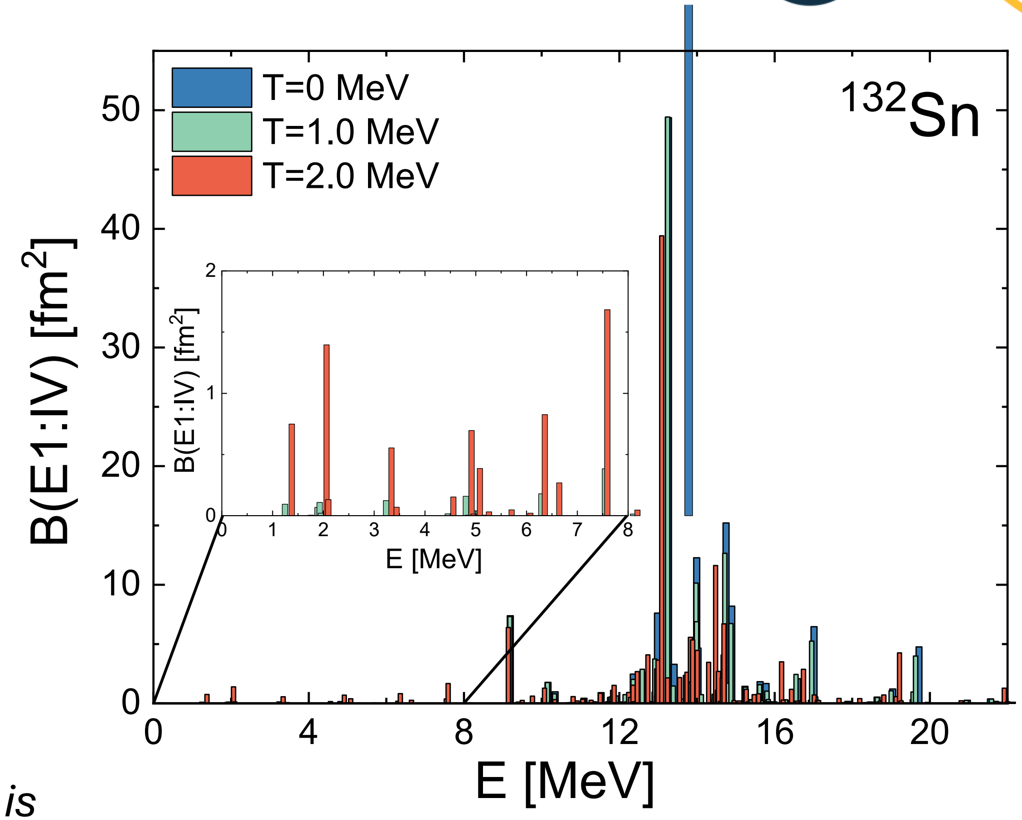

The reduced transition amplitude of a normalized positive-energy mode is

$$\mathcal{M}_{\nu}(Q_J) = \sum_{mi} \boxed{(f_i - f_m)} \left[X^{\nu,J}_{mi} + (-1)^J Y^{\nu,J}_{mi}\right] \langle m \| Q_J \| i \rangle$$

$$= \sum_{mi} \boxed{\sqrt{(f_i - f_m)}} \left[\tilde{X}^{\nu,J}_{mi} + (-1)^J \tilde{Y}^{\nu,J}_{mi}\right] \langle m \| Q_J \| i \rangle.$$

$$\Rightarrow \quad \boxed{B^{\mathrm{abs}}_T(J;\omega_\nu) = |\mathcal{M}_{\nu}(Q_J)|^2.}$$

*E. Yüksel, G. Colò, E. Khan, Y. F. Niu, and K. Bozkurt, Phys. Rev. C 96, 024303, (2017).

FT-HF+BCS: how temperature modifies states and pairing

The paired thermal reference minimizes the grand potential in the space of normal and anomalous densities

$$\Omega[\rho, \kappa, \kappa^*] = E[\rho, \kappa, \kappa^*] - TS - \lambda_n N - \lambda_p Z.$$

Thermal quasiparticles $E_k = \sqrt{(\varepsilon_k - \lambda)^2 + \Delta_k^2}, \qquad f_k = \dfrac{1}{1 + \exp(E_k/T)}.$

Thermal normal density and pairing tensor

$$\rho_k = v_k^2(1 - f_k) + u_k^2 f_k$$

Thermal quasiparticles modify the orbital occupation.

$$\kappa_k = u_k v_k (1 - 2f_k)$$

The factor $1 - 2f_k$ reduces pair coherence.

Self-consistent pairing gap $\Delta_k = -\sum_{k'} V_{kk'}\, u_{k'} v_{k'} \left(1 - 2f_{k'}\right).$

$$\boxed{T \uparrow \quad \Longrightarrow \quad f_k \uparrow \quad \Longrightarrow \quad (1 - 2f_k) \downarrow \quad \Longrightarrow \quad \kappa_k, \Delta_k \downarrow .}$$

$T \to 0: \quad f_k \to 0, \quad \rho_k \to v_k^2, \quad \kappa_k \to u_k v_k. \qquad \Delta \to 0: \quad$ normal FT-HF / FT-RPA limit.

FT-HF+BCS reference $\longrightarrow$ FT-QRPA / FT-PNQRPA

FT-HF+BCS: how temperature modifies states and pairing

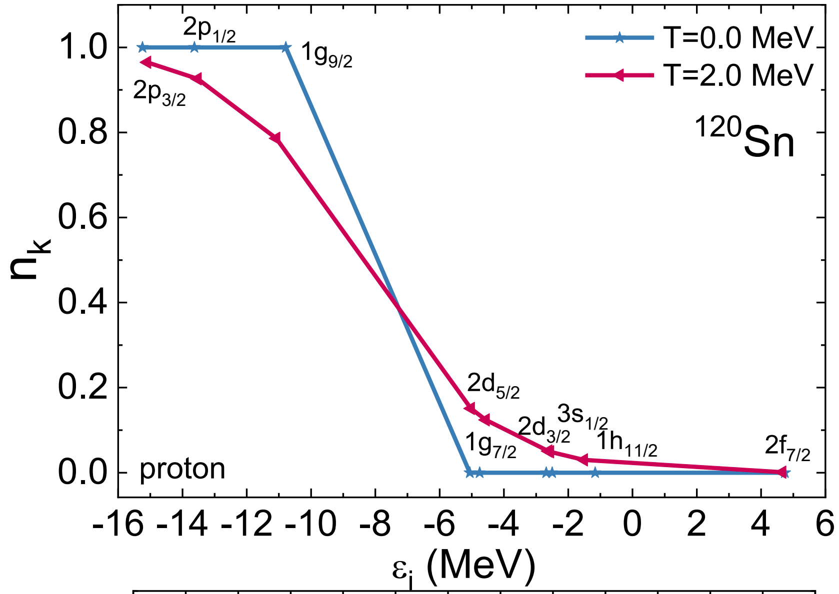

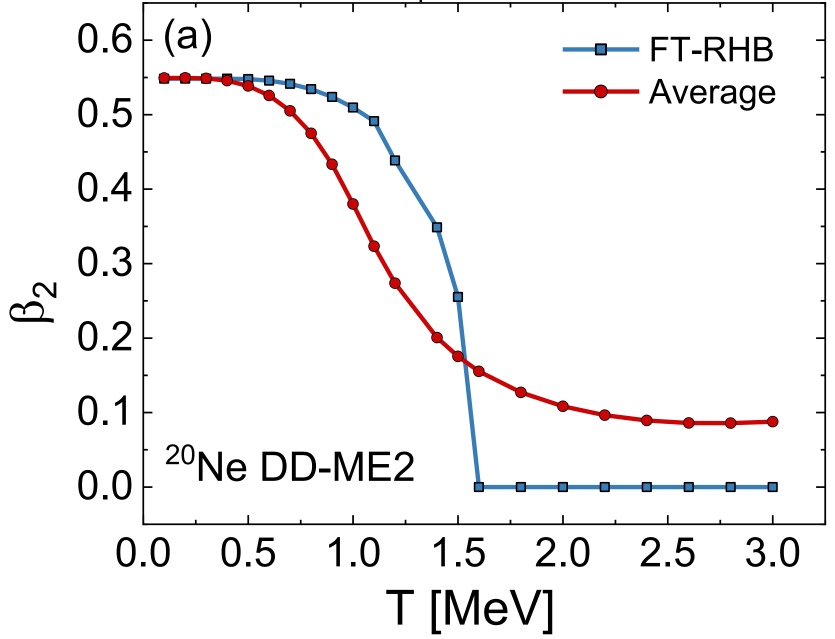

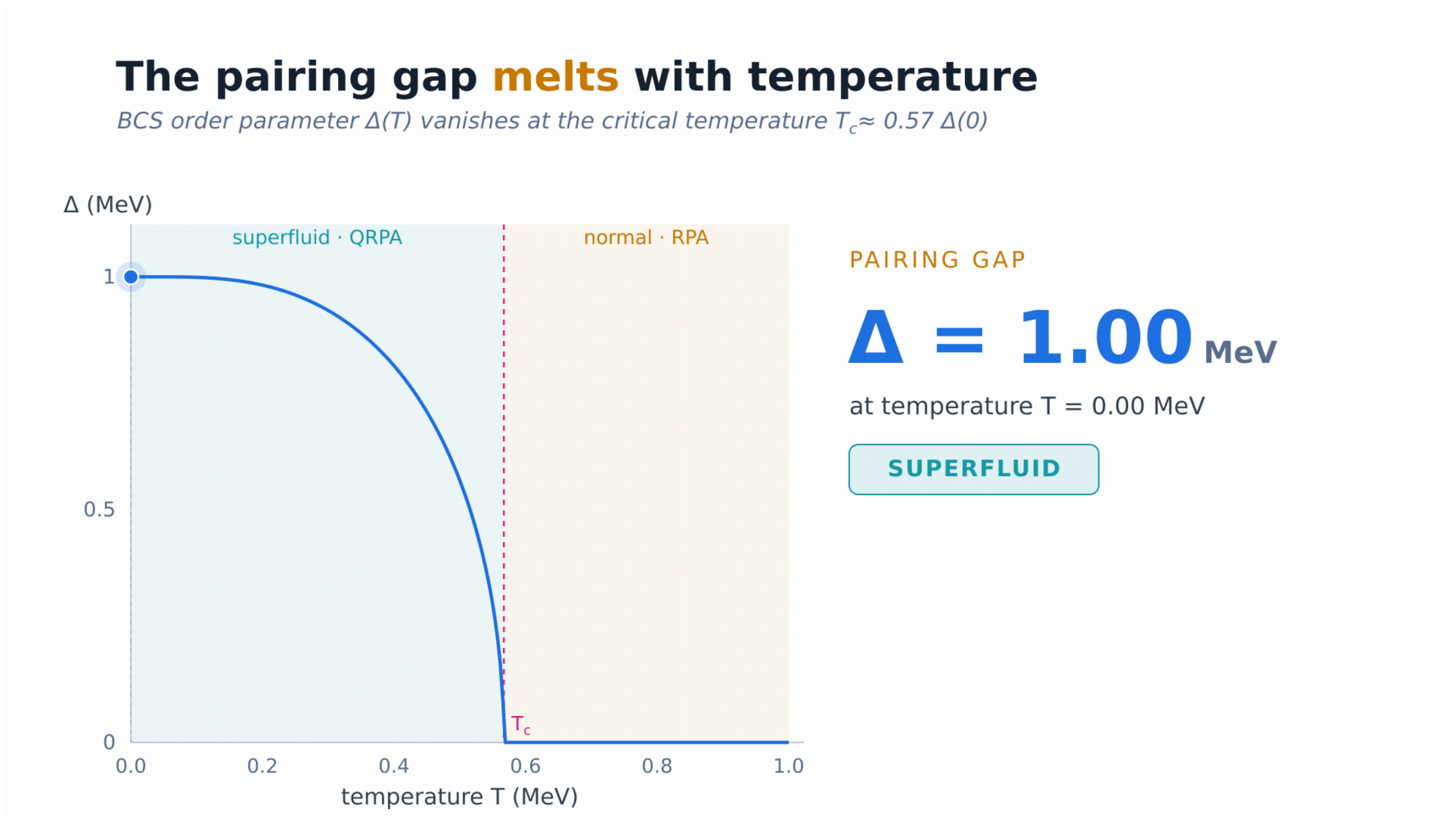

Thermal commutator metrics

- From FT-HF+BCS, define quasiparticle operators

$$\alpha_a^\dagger, \qquad \alpha_a,$$

$$E_a = \sqrt{(\varepsilon_a - \lambda)^2 + \Delta_a^2}.$$

- Fermi–Dirac occupations are

$$f_a = \frac{1}{1+\exp(E_a/T)}.$$

- At finite temperature, the quasiparticle vacuum is replaced by a **thermal ensemble**. In the diagonal quasiparticle basis,

$$\langle \alpha_a^\dagger \alpha_b \rangle_T = \delta_{ab} \boxed{f_a,} \qquad \langle \alpha_a \alpha_b^\dagger \rangle_T = \delta_{ab} \boxed{(1 - f_a)}.$$

- The grand Hamiltonian is written as

$$\hat{\mathcal{H}} = \hat{H} - \lambda \hat{N} = E_{\text{ref}} + \sum_a E_a \alpha_a^\dagger \alpha_a + \hat{V}_{\text{res}}.$$

- **Two-quasiparticle pair sector:** a pair-creation operator and its reverse partner by

$$\mathsf{P}_{ab}^\dagger = \alpha_a^\dagger \alpha_b^\dagger, \qquad \mathsf{P}_{ab} = \alpha_b \alpha_a.$$

- The diagonal Hamiltonian gives

$$[\hat{\mathcal{H}}_0, \mathsf{P}_{ab}^\dagger] = (E_a + E_b)\mathsf{P}_{ab}^\dagger.$$

- **Thermal quasiparticle-scattering sector:** we define the scattering operator and its reverse partner by

$$\mathsf{S}_{ab}^\dagger = \alpha_a^\dagger \alpha_b, \qquad \mathsf{S}_{ab} = \alpha_b^\dagger \alpha_a.$$

- The diagonal Hamiltonian gives

$$[\hat{\mathcal{H}}_0, \mathsf{S}_{ab}^\dagger] = (E_a - E_b)\mathsf{S}_{ab}^\dagger.$$

Thermal commutator metrics

- From FT-HF+BCS, define quasiparticle operators

$$\alpha_a^\dagger, \qquad \alpha_a,$$

$$E_a = \sqrt{(\varepsilon_a - \lambda)^2 + \Delta_a^2}.$$

- Fermi–Dirac occupations are

$$f_a = \frac{1}{1+\exp(E_a/T)}.$$

- At finite temperature, the quasiparticle vacuum is replaced by a **thermal ensemble**. In the diagonal quasiparticle basis,

$$\langle \alpha_a^\dagger \alpha_b \rangle_T = \delta_{ab} \boxed{f_a}, \qquad \langle \alpha_a \alpha_b^\dagger \rangle_T = \delta_{ab} \boxed{(1-f_a)}.$$

- The grand Hamiltonian is written as

$$\hat{\mathcal{H}} = \hat{H} - \lambda \hat{N} = E_{\mathrm{ref}} + \sum_a E_a \alpha_a^\dagger \alpha_a + \hat{V}_{\mathrm{res}}.$$

- The thermal metrics are the FT-QRPA analogue of the FT-RPA factor fi − fm.

$$\mathsf{P}_{ab}^\dagger = \alpha_a^\dagger \alpha_b^\dagger, \qquad \mathsf{P}_{ab} = \alpha_b \alpha_a.$$

$$\begin{aligned}
\left\langle [\mathsf{P}_{ab}, \mathsf{P}_{ab}^\dagger] \right\rangle_T &= \left\langle \alpha_b \alpha_a \alpha_a^\dagger \alpha_b^\dagger - \alpha_a^\dagger \alpha_b^\dagger \alpha_b \alpha_a \right\rangle_T \\
&= \langle (1-\hat{n}_a)(1-\hat{n}_b) - \hat{n}_a \hat{n}_b \rangle_T \\
&= (1-f_a)(1-f_b) - f_a f_b \\
&= \boxed{1 - f_a - f_b}.
\end{aligned}$$

$$\mathsf{S}_{ab}^\dagger = \alpha_a^\dagger \alpha_b, \qquad \mathsf{S}_{ab} = \alpha_b^\dagger \alpha_a.$$

$$\begin{aligned}
\left\langle [\mathsf{S}_{ab}, \mathsf{S}_{ab}^\dagger] \right\rangle_T &= \left\langle \alpha_b^\dagger \alpha_a \alpha_a^\dagger \alpha_b - \alpha_a^\dagger \alpha_b \alpha_b^\dagger \alpha_a \right\rangle_T \\
&= \langle \hat{n}_b (1-\hat{n}_a) - \hat{n}_a (1-\hat{n}_b) \rangle_T \\
&= f_b(1-f_a) - f_a(1-f_b) \\
&= \boxed{f_b - f_a}.
\end{aligned}$$

$\hat{n}_a = \alpha_a^\dagger \alpha_a$ is a quasiparticle-number operator and that $\alpha_a \alpha_a^\dagger = 1 - \hat{n}_a$.

Thermal commutators

- The thermal metrics are the FT-QRPA analogue of the FT-RPA factor fi − fm.

$$\left\langle [\mathsf{P}_{ab}, \mathsf{P}^\dagger_{ab}] \right\rangle_T = \left\langle \alpha_b\alpha_a\alpha^\dagger_a\alpha^\dagger_b - \alpha^\dagger_a\alpha^\dagger_b\alpha_b\alpha_a \right\rangle_T$$
$$= \langle (1-\hat{n}_a)(1-\hat{n}_b) - \hat{n}_a\hat{n}_b \rangle_T$$
$$= (1-f_a)(1-f_b) - f_a f_b$$
$$= \boxed{1 - f_a - f_b}.$$

$$\left\langle [\mathsf{S}_{ab}, \mathsf{S}^\dagger_{ab}] \right\rangle_T = \left\langle \alpha^\dagger_b\alpha_a\alpha^\dagger_a\alpha_b - \alpha^\dagger_a\alpha_b\alpha^\dagger_b\alpha_a \right\rangle_T$$
$$= \langle \hat{n}_b(1-\hat{n}_a) - \hat{n}_a(1-\hat{n}_b) \rangle_T$$
$$= f_b(1-f_a) - f_a(1-f_b)$$
$$= \boxed{f_b - f_a}.$$

$\hat{n}_a = \alpha^\dagger_a\alpha_a$ is a quasiparticle-number operator and that $\alpha_a\alpha^\dagger_a = 1 - \hat{n}_a$.

- **FT-QRPA phonon operator**: A collective FT-QRPA excitation contains both pair and thermal-

$$\mathsf{P}^\dagger_{ab} = \alpha^\dagger_a\alpha^\dagger_b, \qquad \mathsf{P}_{ab} = \alpha_b\alpha_a.$$
$$\mathsf{S}^\dagger_{ab} = \alpha^\dagger_a\alpha_b, \qquad \mathsf{S}_{ab} = \alpha^\dagger_b\alpha_a.$$

$$\Gamma^\dagger_\nu = \sum_{a\le b}\left(X^\nu_{ab}\mathsf{P}^\dagger_{ab} - Y^\nu_{ab}\mathsf{P}_{ab}\right) + \boxed{\sum_{E_a>E_b}\left(P^\nu_{ab}\mathsf{S}^\dagger_{ab} - Q^\nu_{ab}\mathsf{S}_{ab}\right)}.$$

- X, Y are forward and backward pair amplitudes;
- P, Q are forward and reverse thermal-scattering amplitudes;

Projected equation of motion

- The finite-temperature equation of motion is

$$\left\langle [\delta\mathcal{O}, [\hat{\mathcal{H}}, \Gamma_\nu^\dagger]] \right\rangle_T = E_\nu \left\langle [\delta\mathcal{O}, \Gamma_\nu^\dagger] \right\rangle_T, \qquad \hat{\mathcal{H}} = \hat{H} - \lambda\hat{N} = E_{\text{ref}} + \sum_a E_a \alpha_a^\dagger \alpha_a + \hat{V}_{\text{res}}.$$

- project with the four elementary operators. The corresponding right-hand sides are

$$\left\langle [\mathsf{S}_{ab}, \Gamma_\nu^\dagger] \right\rangle_T = (f_b - f_a) P_{ab}^\nu,$$
$$\left\langle [\mathsf{P}_{ab}, \Gamma_\nu^\dagger] \right\rangle_T = (1 - f_a - f_b) X_{ab}^\nu,$$
$$\left\langle [\mathsf{P}_{ab}, \Gamma_\nu^\dagger] \right\rangle_T = (1 - f_a - f_b) Y_{ab}^\nu,$$
$$\left\langle [\mathsf{S}_{ab}, \Gamma_\nu^\dagger] \right\rangle_T = (f_b - f_a) Q_{ab}^\nu.$$

Projected equation of motion

- The finite-temperature equation of motion is

$$\left\langle [\delta\mathcal{O}, [\hat{\mathcal{H}}, \Gamma^\dagger_\nu]] \right\rangle_T = E_\nu \left\langle [\delta\mathcal{O}, \Gamma^\dagger_\nu] \right\rangle_T, \qquad \hat{\mathcal{H}} = \hat{H} - \lambda\hat{N} = E_{\text{ref}} + \sum_a E_a \alpha^\dagger_a \alpha_a + \hat{V}_{\text{res}}.$$

- project with the four elementary operators. The corresponding leftt-hand sides are

$$\mathcal{A}_{ab,cd} \equiv \left\langle [\mathsf{P}_{ab}, [\hat{\mathcal{H}}, \mathsf{P}^\dagger_{cd}]] \right\rangle_T, \qquad \mathcal{B}_{ab,cd} \equiv -\left\langle [\mathsf{P}_{ab}, [\hat{\mathcal{H}}, \mathsf{P}_{cd}]] \right\rangle_T,$$

$$\mathcal{C}_{ab,cd} \equiv \left\langle [\mathsf{S}_{ab}, [\hat{\mathcal{H}}, \mathsf{S}^\dagger_{cd}]] \right\rangle_T, \qquad \mathcal{D}_{ab,cd} \equiv -\left\langle [\mathsf{S}_{ab}, [\hat{\mathcal{H}}, \mathsf{S}_{cd}]] \right\rangle_T,$$

$$a_{ab,cd} \equiv \left\langle [\mathsf{S}_{ab}, [\hat{\mathcal{H}}, \mathsf{P}^\dagger_{cd}]] \right\rangle_T, \qquad b_{ab,cd} \equiv -\left\langle [\mathsf{S}_{ab}, [\hat{\mathcal{H}}, \mathsf{P}_{cd}]] \right\rangle_T,$$

$$a^+_{ab,cd} \equiv \left\langle [\mathsf{P}_{ab}, [\hat{\mathcal{H}}, \mathsf{S}^\dagger_{cd}]] \right\rangle_T, \qquad b^T_{ab,cd} \equiv -\left\langle [\mathsf{P}_{ab}, [\hat{\mathcal{H}}, \mathsf{S}_{cd}]] \right\rangle_T.$$

$$[\hat{\mathcal{H}}_0, \mathsf{P}^\dagger_{ab}] = (E_a + E_b)\mathsf{P}^\dagger_{ab},$$ pair configurations

$$[\hat{\mathcal{H}}_0, \mathsf{S}^\dagger_{ab}] = (E_a - E_b)\mathsf{S}^\dagger_{ab}.$$ thermal-scattering configurations

Projected equation of motion

- The diagonal quasiparticle Hamiltonian gives

$$[\hat{\mathcal{H}}_0, \mathsf{P}^\dagger_{ab}] = (E_a + E_b)\mathsf{P}^\dagger_{ab},$$
$$[\hat{\mathcal{H}}_0, \mathsf{S}^\dagger_{ab}] = (E_a - E_b)\mathsf{S}^\dagger_{ab}.$$

- Consequently, the diagonal pieces occur only in the forward pair and forward scattering blocks:

$$\mathcal{A}_{ab,cd} = (1 - f_a - f_b)(E_a + E_b)\delta_{ac}\delta_{bd} + \text{residual part},$$
$$\mathcal{C}_{ab,cd} = (f_b - f_a)(E_a - E_b)\delta_{ac}\delta_{bd} + \text{residual part}.$$

Thermal Wick factorization gives the directly projected blocks:

$$\mathcal{A}_{ab,cd} = (1 - f_a - f_b)(E_a + E_b)\delta_{ac}\delta_{bd} + (1 - f_a - f_b)(1 - f_c - f_d)A'_{ab,cd}.$$
$$\mathcal{B}_{ab,cd} = (1 - f_a - f_b)(1 - f_c - f_d)B_{ab,cd}.$$
$$\mathcal{C}_{ab,cd} = (f_b - f_a)(E_a - E_b)\delta_{ac}\delta_{bd} + (f_b - f_a)(f_d - f_c)C'_{ab,cd},$$
$$\mathcal{D}_{ab,cd} = (f_b - f_a)(f_d - f_c)D_{ab,cd}.$$
$$a^{(\mathrm{proj})}_{ab,cd} = (f_b - f_a)(1 - f_c - f_d)\, a_{ab,cd},$$
$$b^{(\mathrm{proj})}_{ab,cd} = (f_b - f_a)(1 - f_c - f_d)\, b_{ab,cd}.$$

FT-QRPA MATRIX

$$\begin{aligned}A'_{\alpha\beta\gamma\delta} &= \Big(u_\alpha u_\beta u_\gamma u_\delta + v_\alpha v_\beta v_\gamma v_\delta\Big)\mathcal{V}_{\alpha\beta\gamma\delta} \\ &+ \Big(u_\alpha v_\beta u_\gamma v_\delta + v_\alpha u_\beta v_\gamma u_\delta\Big)\mathcal{V}_{\alpha\bar{\delta}\bar{\beta}\gamma} \\ &- \Big(u_\alpha v_\beta v_\gamma u_\delta + v_\alpha u_\beta u_\gamma v_\delta\Big)\mathcal{V}_{\alpha\bar{\gamma}\bar{\beta}\delta},\end{aligned}$$

$$\begin{aligned}B_{\alpha\beta\gamma\delta} &= \Big(u_\alpha v_\beta v_\gamma u_\delta + v_\alpha u_\beta u_\gamma v_\delta\Big)\mathcal{V}_{\alpha\delta\bar{\gamma}\bar{\beta}} \\ &+ \Big(u_\alpha v_\beta u_\gamma v_\delta + v_\alpha u_\beta v_\gamma u_\delta\Big)\mathcal{V}_{\alpha\gamma\bar{\beta}\bar{\delta}} \\ &- \Big(u_\alpha u_\beta v_\gamma v_\delta + v_\alpha v_\beta u_\gamma u_\delta\Big)\mathcal{V}_{\alpha\beta\bar{\gamma}\bar{\delta}}.\end{aligned}$$

$$\begin{aligned}a_{\alpha\beta\gamma\delta} &= \Big(v_\alpha u_\beta u_\gamma v_\delta - u_\alpha v_\beta v_\gamma u_\delta\Big)\mathcal{V}_{\alpha\beta\gamma\delta} \\ &- \Big(v_\alpha v_\beta u_\gamma v_\delta - u_\alpha u_\beta v_\gamma u_\delta\Big)\mathcal{V}_{\alpha\delta\beta\bar{\gamma}} \\ &+ \Big(v_\alpha v_\beta v_\gamma u_\delta - u_\alpha u_\beta u_\gamma v_\delta\Big)\mathcal{V}_{\alpha\gamma\bar{\beta}\bar{\delta}},\end{aligned}$$

$$\begin{aligned}C'_{\alpha\beta\gamma\delta} &= \Big(u_\alpha u_\beta u_\gamma u_\delta + v_\alpha v_\beta v_\gamma v_\delta\Big)\mathcal{V}_{\alpha\delta\beta\gamma} \\ &- \Big(u_\alpha v_\beta u_\gamma v_\delta + v_\alpha u_\beta v_\gamma u_\delta\Big)\mathcal{V}_{\alpha\bar{\beta}\bar{\delta}\gamma} \\ &+ \Big(u_\alpha u_\beta v_\gamma v_\delta + v_\alpha v_\beta u_\gamma u_\delta\Big)\mathcal{V}_{\alpha\bar{\gamma}\bar{\delta}\beta},\end{aligned}$$

$$\begin{aligned}D_{\alpha\beta\gamma\delta} &= \Big(u_\alpha u_\beta u_\gamma u_\delta + v_\alpha v_\beta v_\gamma v_\delta\Big)\mathcal{V}_{\alpha\beta\gamma\delta} \\ &- \Big(u_\alpha v_\beta v_\gamma u_\delta + v_\alpha u_\beta u_\gamma v_\delta\Big)\mathcal{V}_{\alpha\bar{\beta}\bar{\gamma}\delta} \\ &+ \Big(u_\alpha u_\beta v_\gamma v_\delta + v_\alpha v_\beta u_\gamma u_\delta\Big)\mathcal{V}_{\alpha\delta\bar{\gamma}\bar{\beta}},\end{aligned}$$

$$\begin{aligned}b_{\alpha\beta\gamma\delta} &= \Big(v_\alpha u_\beta u_\gamma u_\delta - u_\alpha v_\beta v_\gamma v_\delta\Big)\mathcal{V}_{\bar{\alpha}\beta\gamma\delta} \\ &- \Big(v_\alpha v_\beta u_\gamma v_\delta - u_\alpha u_\beta v_\gamma u_\delta\Big)\mathcal{V}_{\alpha\delta\beta\bar{\gamma}} \\ &+ \Big(v_\alpha v_\beta v_\gamma u_\delta - u_\alpha u_\beta u_\gamma v_\delta\Big)\mathcal{V}_{\alpha\gamma\bar{\beta}\bar{\delta}}.\end{aligned}$$

FT-QRPA MATRIX

- In the normalized basis, the FT-QRPA equation has the canonical form

$$\boxed{\begin{pmatrix} \widetilde{C} & \widetilde{a} & \widetilde{b} & \widetilde{D} \\ \widetilde{a}^\dagger & \widetilde{A} & \widetilde{B} & \widetilde{b}^T \\ -\widetilde{b}^\dagger & -\widetilde{B}^* & -\widetilde{A}^* & -\widetilde{a}^T \\ -\widetilde{D}^* & -\widetilde{b}^* & -\widetilde{a}^* & -\widetilde{C}^* \end{pmatrix} \begin{pmatrix} \widetilde{P}^\nu \\ \widetilde{X}^\nu \\ \widetilde{Y}^\nu \\ \widetilde{Q}^\nu \end{pmatrix} = E_\nu \begin{pmatrix} \widetilde{P}^\nu \\ \widetilde{X}^\nu \\ \widetilde{Y}^\nu \\ \widetilde{Q}^\nu \end{pmatrix} .}$$

- The canonical blocks are

$$\widetilde{A}_{ab,cd} = (E_a + E_b)\delta_{ac}\delta_{bd} + \sqrt{(1 - f_a - f_b)(1 - f_c - f_d)}A'_{ab,cd},$$

$$\widetilde{B}_{ab,cd} = \sqrt{(1 - f_a - f_b)(1 - f_c - f_d)}B_{ab,cd},$$

$$\widetilde{C}_{ab,cd} = (E_a - E_b)\delta_{ac}\delta_{bd} + \sqrt{(f_b - f_a)(f_d - f_c)}C'_{ab,cd},$$

$$\widetilde{D}_{ab,cd} = \sqrt{(f_b - f_a)(f_d - f_c)}D_{ab,cd},$$

$$\widetilde{a}_{ab,cd} = \sqrt{(f_b - f_a)(1 - f_c - f_d)}a_{ab,cd},$$

$$\widetilde{b}_{ab,cd} = \sqrt{(f_b - f_a)(1 - f_c - f_d)}b_{ab,cd}.$$

$$\widetilde{X}^\nu_{ab} = X^\nu_{ab}\sqrt{1 - f_a - f_b},$$
$$\widetilde{P}^\nu_{ab} = P^\nu_{ab}\sqrt{f_b - f_a},$$

$$\widetilde{Y}^\nu_{ab} = Y^\nu_{ab}\sqrt{1 - f_a - f_b},$$
$$\widetilde{Q}^\nu_{ab} = Q^\nu_{ab}\sqrt{f_b - f_a}.$$

Normalization and strength function

Their normalization is fixed by the thermal boson condition

$$\left\langle [\Gamma_\nu, \Gamma^\dagger_{\nu'}] \right\rangle_T = \delta_{\nu\nu'}.$$

$$\delta_{\nu\nu'} = \sum_{a\le b} \left[\widetilde{X}^{\nu *}_{ab} \widetilde{X}^{\nu'}_{ab} - \widetilde{Y}^{\nu *}_{ab} \widetilde{Y}^{\nu'}_{ab} \right] + \sum_{E_a > E_b} \left[\widetilde{P}^{\nu *}_{ab} \widetilde{P}^{\nu'}_{ab} - \widetilde{Q}^{\nu *}_{ab} \widetilde{Q}^{\nu'}_{ab} \right].$$

$$\boxed{\sum_{a\le b} \left(|\widetilde{X}^{\nu}_{ab}|^2 - |\widetilde{Y}^{\nu}_{ab}|^2 \right) + \sum_{E_a > E_b} \left(|\widetilde{P}^{\nu}_{ab}|^2 - |\widetilde{Q}^{\nu}_{ab}|^2 \right) = 1.}$$

$$\boxed{\begin{aligned} B(\mathrm{T}J, w) = \left| \langle w || \hat{F}_J || \widetilde{0} \rangle \right|^2 = \Bigg| \sum_{c \ge d} \Big\{ & (\widetilde{X}^w_{cd} + (-1)^{j_c - j_d + J} \widetilde{Y}^w_{cd})(u_c v_d + (-1)^J v_c u_d) \sqrt{1 - f_c - f_d} \\ & + (\widetilde{P}^w_{cd} + (-1)^{j_c - j_d + J} \widetilde{Q}^w_{cd})(u_c u_d - (-1)^J v_c v_d) \sqrt{f_d - f_c} \Big\} \langle c || \hat{F}_J || d \rangle \Bigg|^2, \end{aligned}}$$

Consistency checks

Zero-temperature limit

For $T \to 0$,

$$f_a \to 0, \qquad 1 - f_a - f_b \to 1, \qquad f_b - f_a \to 0.$$

Hence

$$\widetilde{P}, \widetilde{Q} \to 0, \qquad \widetilde{C}, \widetilde{D}, \widetilde{a}, \widetilde{b} \to 0,$$

and the FT-QRPA matrix reduces to ordinary QRPA.

Vanishing pairing limit

When

$$\Delta \to 0,$$

the Bogoliubov coefficients become particle-like or hole-like:

$$u^2 \to 0 \text{ or } 1, \qquad v^2 \to 1 \text{ or } 0.$$

The full paired configuration space then reorganizes into the normal FT-RPA or FT-PNRPA transition space. The mapping is a property of the complete assembled response matrix, not of one individual QRPA block alone.

Isovector dipole excitations at finite temperatures

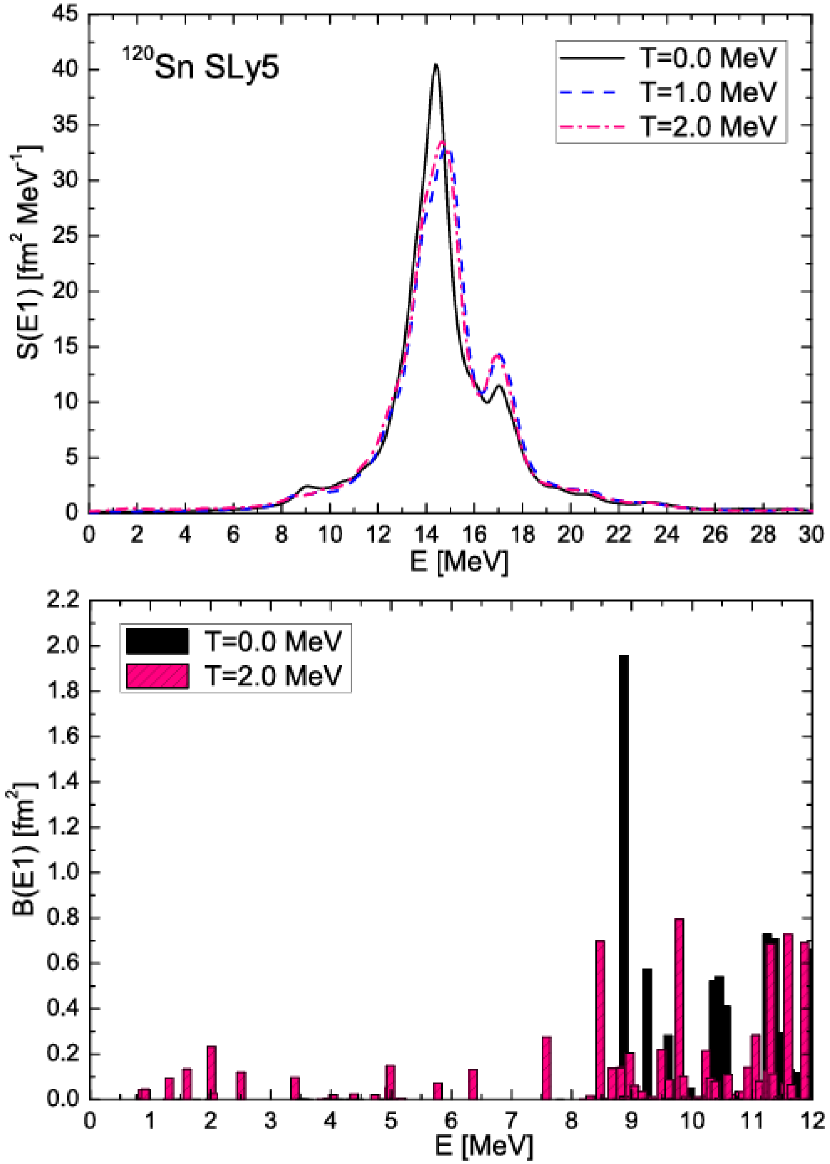

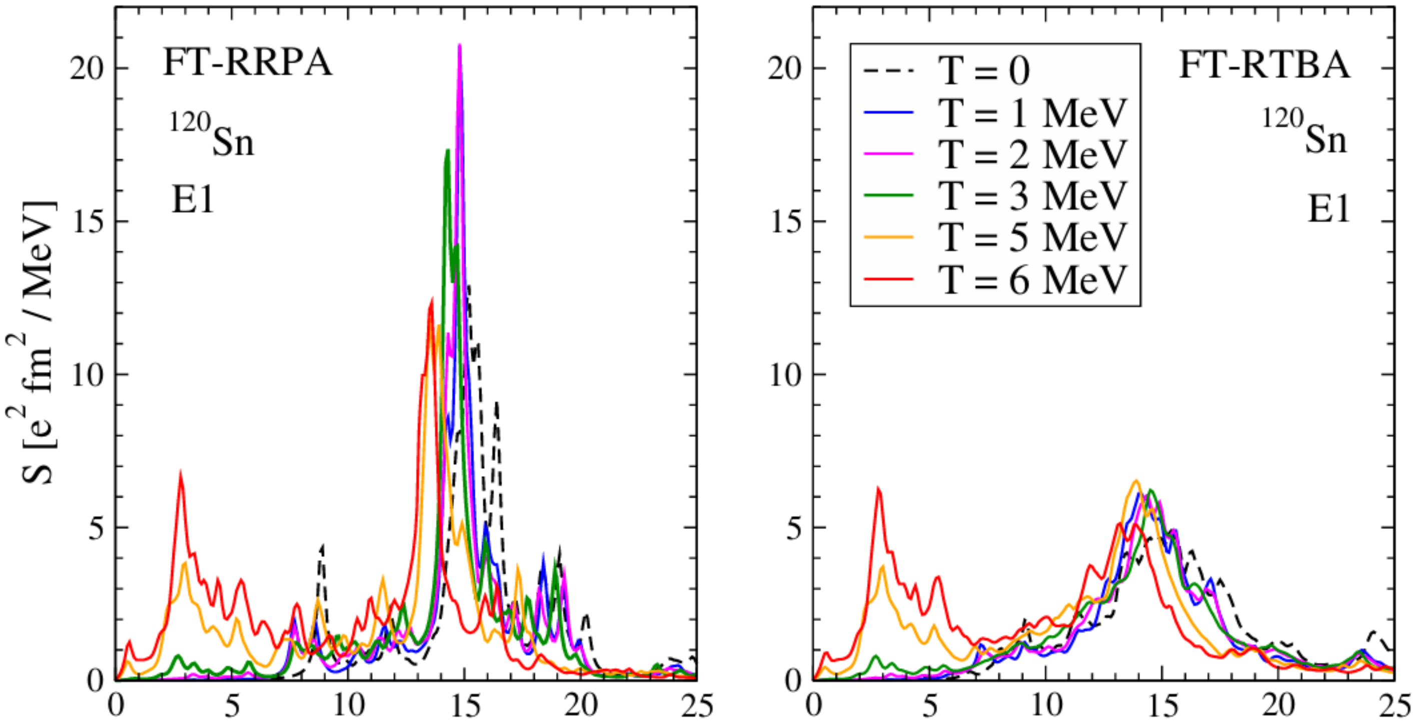

Isoscalar quadrupole excitations at finite temperatures

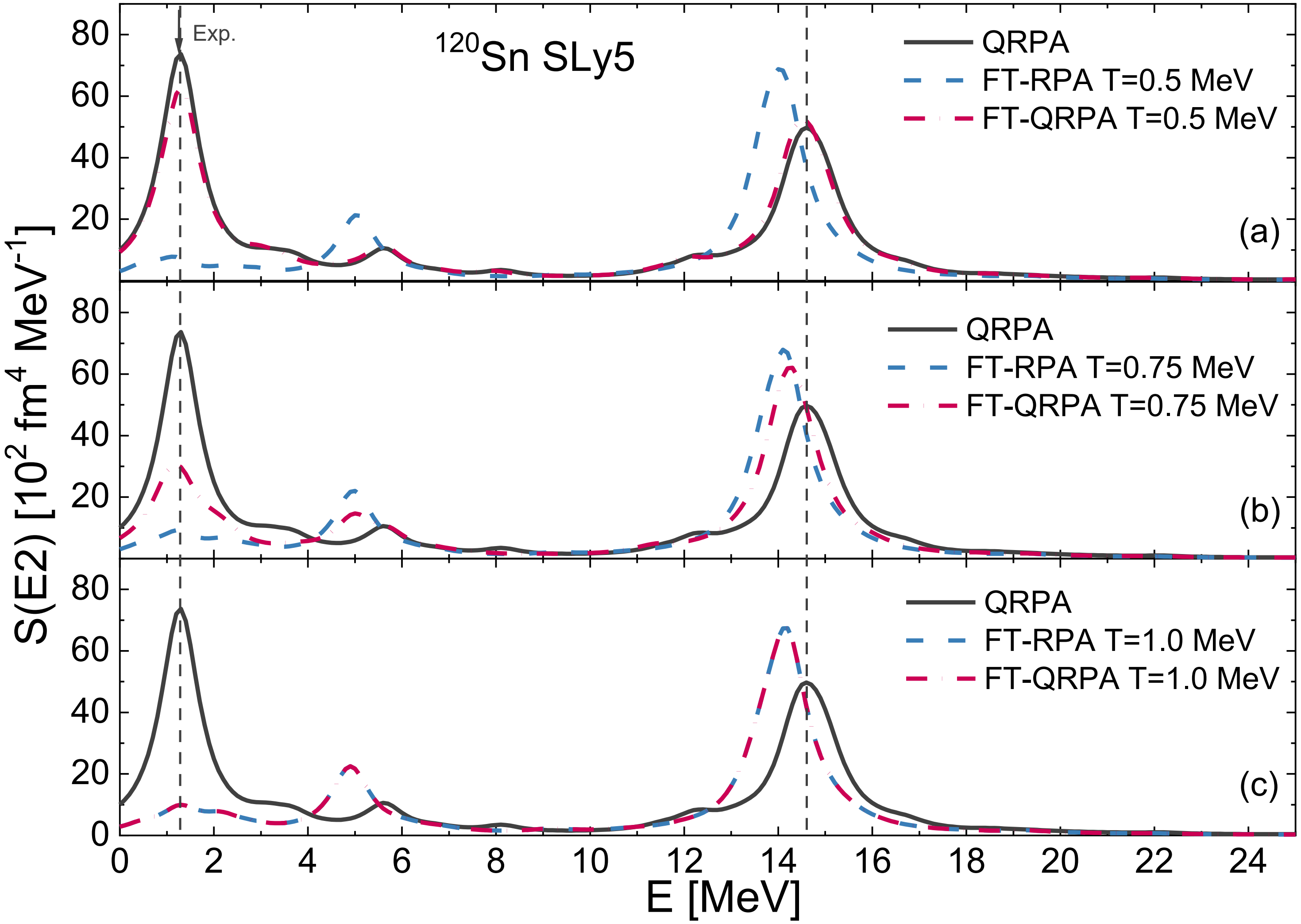

- ✓ *FT-RPA and FT-QRPA results are quite different both in the high-energy and low-energy regions.*
- ✓ *This difference indicates the important role of pairing correlations in open-shell nuclei at finite temperatures.*

E. Yüksel, G. Colò, E. Khan, Y. F. Niu, and K. Bozkurt, Phys. Rev. C 96, 024303, (2017).

The isoscalar quadrupole response in ^{120}Sn using the FT-Q(RPA) and SLy5 interaction at finite temperatures.

Isoscalar monopole excitations at finite temperatures

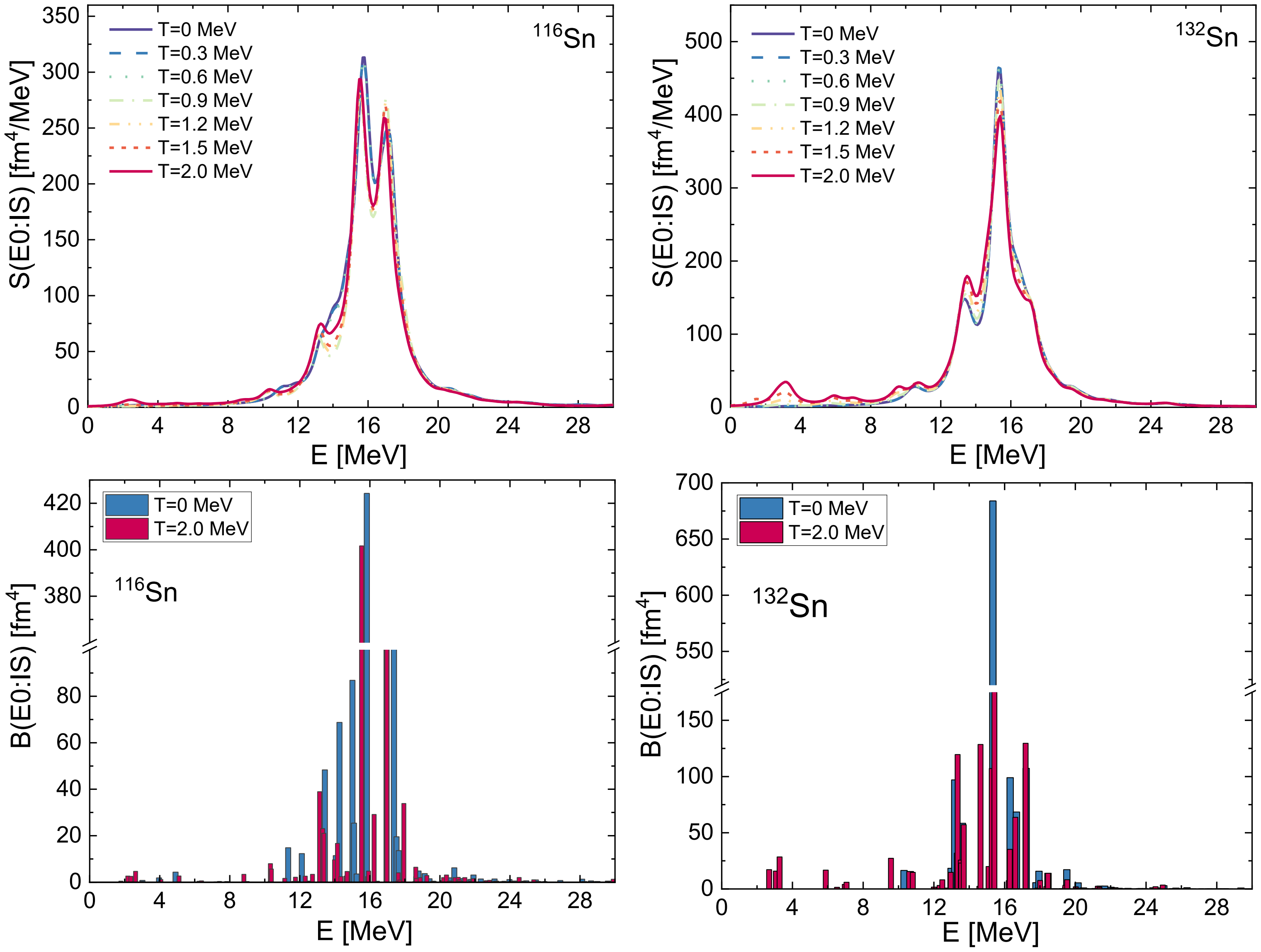

Isoscalar monopole response in 116Sn and 132Sn nuclei with increasing temperature. The calculations are performed using the SkM interaction.*

- *The isoscalar monopole strength is not sensitive to the temperature effects up to T=0.9 MeV.*
- *Even at higher temperatures, the ISGMR peak is slightly modified, whereas collectivity is destroyed.*
- *In addition, new excited states are obtained below E<10 MeV with increasing temperature.*
- *Low-energy region of the ^{132}Sn is more sensitive to the changes in the temperature compared to ^{116}Sn.*

PHYSICAL REVIEW C **112**, L051304 (2025)

Letter

Hot pygmy dipole strength in nickel isotopes

Amandeep Kaur [1,*] Esra Yüksel [2,†] and Nils Paar [1,‡]
[1] Department of Physics, Faculty of Science, University of Zagreb, Bijenička c. 32, 10000 Zagreb, Croatia
[2] School of Mathematics and Physics, University of Surrey, Guildford, Surrey GU2 7XH, United Kingdom

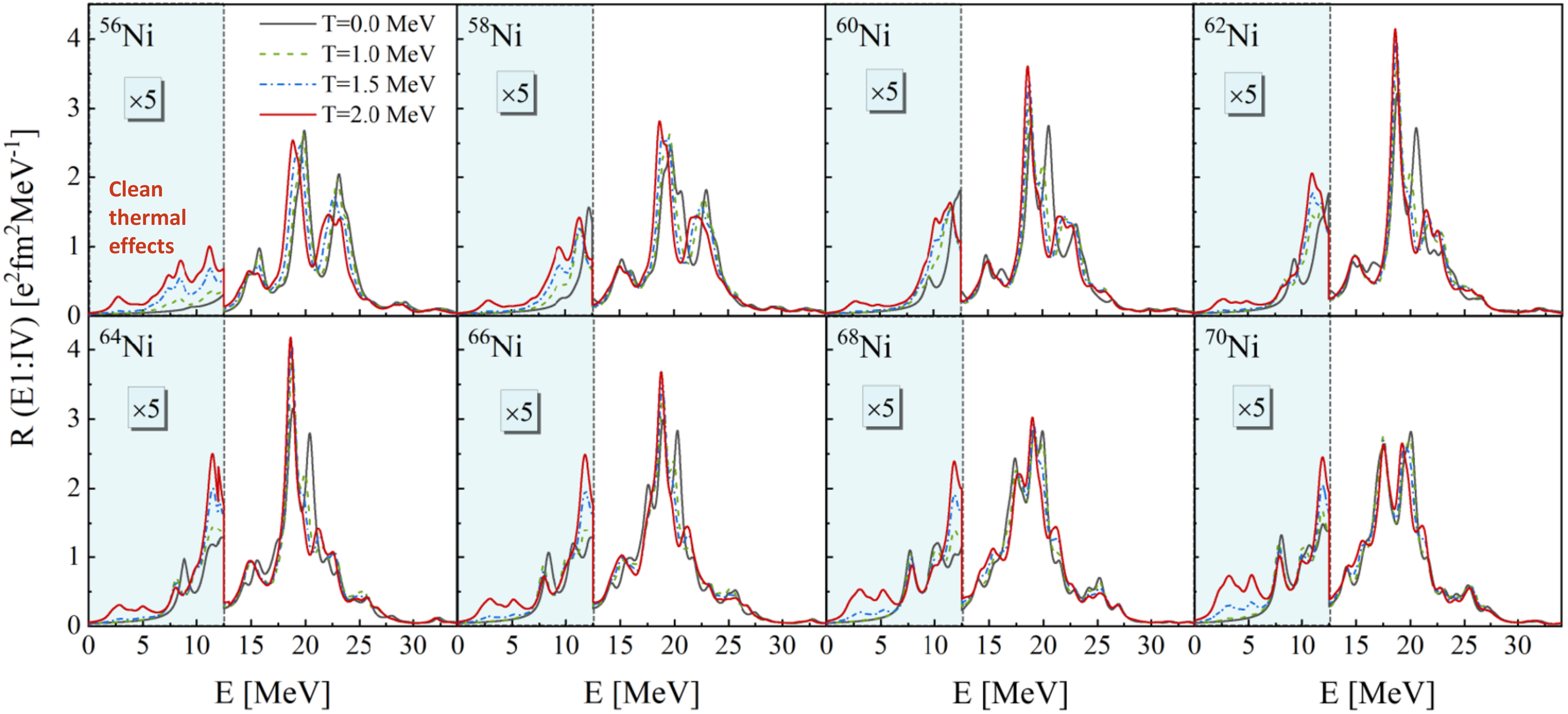

Hot pygmy dipole strength in nickel isotopes

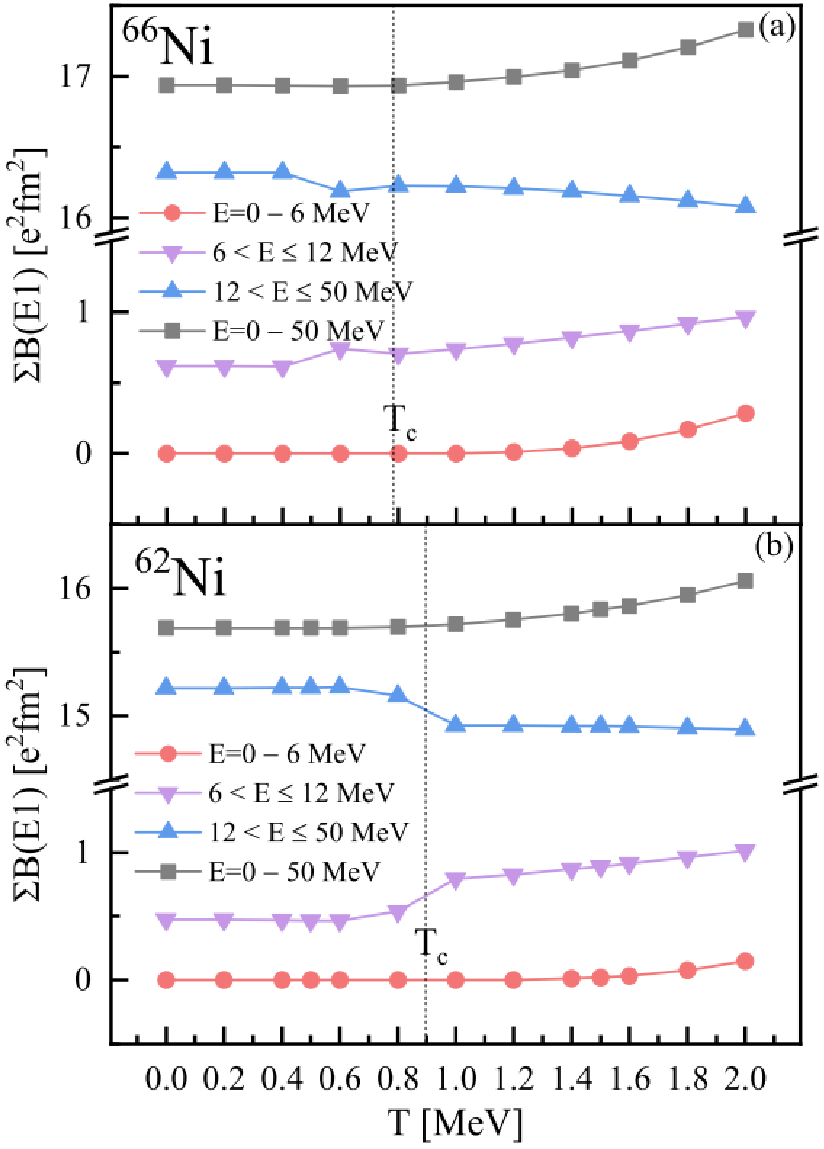

Integrated E1 strength ΣB(E1) for 66Ni (a) and 62Ni (b) as a function of temperature.

1. **Low temperatures (T < Tc)**:
   - Pairing correlations are still active; thermal occupation factors remain small. The E1 strength changes only weakly.

2. **Around the pairing critical temperature (Tc)**:
   - Clear onset of strength redistribution.
   - Pairing collapse enables thermal unblocking of new transitions.

3. **High temperatures (T ≳ 1–2 MeV)**:
   - Strong increase of E1 strength in the 6–12 MeV region.
   - Simultaneous reduction of GDR-region strength, indicating transfer rather than simple broadening.
   - Confirms that **HPDS arises mainly from redistribution of strength from high to low energies**.

* Amandeep Kaur, Esra Yüksel and Nils Paar Phys. Rev. C 112, L051304, (2025).

PHYSICAL REVIEW C **112**, 014307 (2025)

Electric and magnetic γ-ray strength functions at finite temperature

Amandeep Kaur[1,*], Esra Yüksel[2,†] and Nils Paar[1,‡]
[1]Department of Physics, Faculty of Science, University of Zagreb, Bijenička c. 32, 10000 Zagreb, Croatia
[2]School of Mathematics and Physics, University of Surrey, Guildford, Surrey GU2 7XH, United Kingdom

(Received 16 January 2025; accepted 17 June 2025; published 2 July 2025)

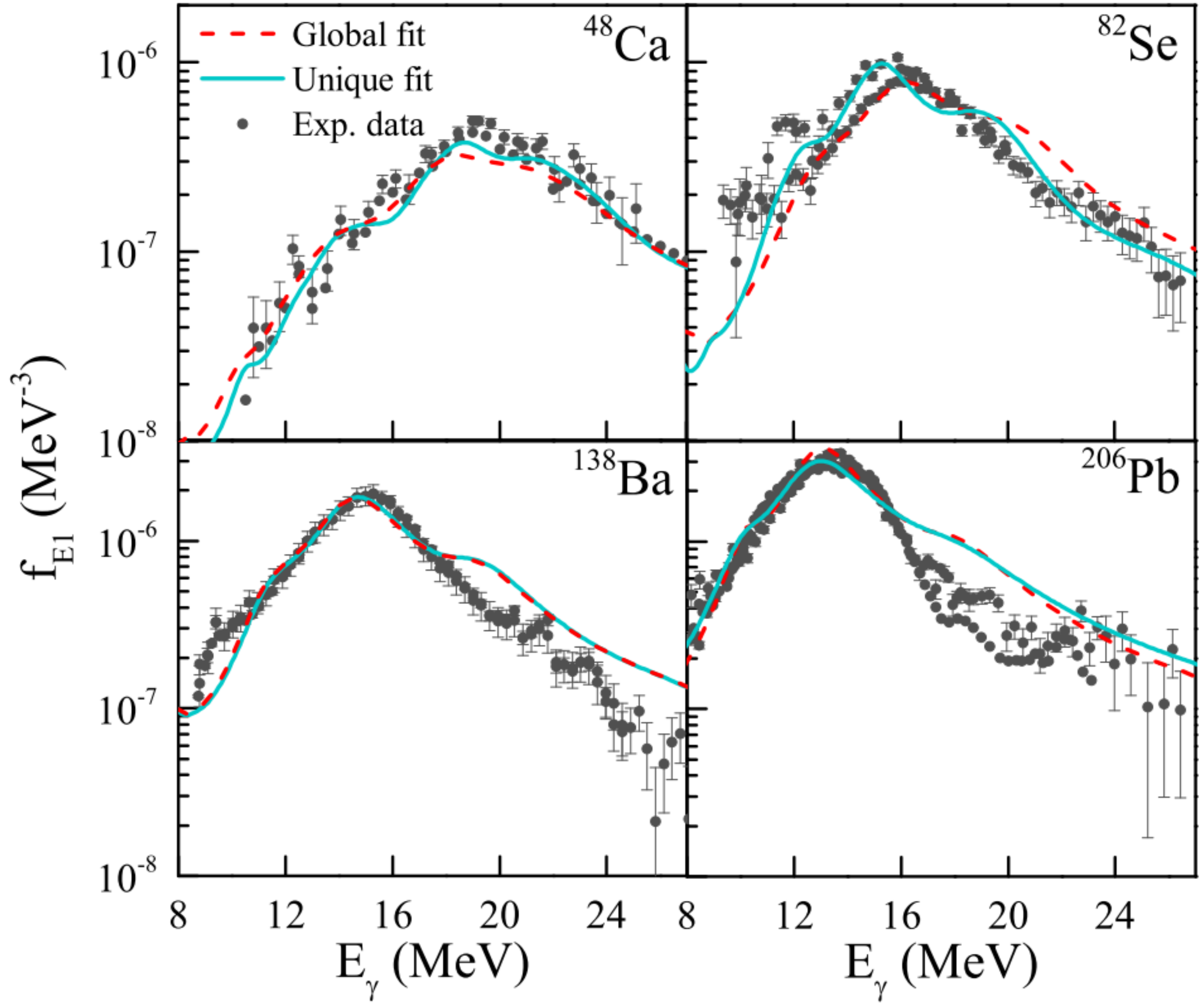

Benchmarking the zero-temperature E1 γ-strength function

- Benchmark at T=0: RQRPA E1 γSFs reproduce photoabsorption data.
- Dataset: 42 spherical and near-spherical nuclei, A=40–208.
- Spreading effects: included through fitted global/unique width prescriptions.
- Next step: extend to finite-temperature E1+M1 γSFs.

$$f_{E1}(E) = \frac{16\pi e^2}{27\hbar^3 c^3} \times R_{E1}(E).$$

$$f_{M1}(E) = \frac{16\pi}{27\hbar^3 c^3} \frac{\Gamma/2\pi}{((E-w)^2+\Gamma^2/4)} B(M1),$$

PHYSICAL REVIEW C **112**, 014307 (2025)

Electric and magnetic γ-ray strength functions at finite temperature

Amandeep Kaur[1,*] Esra Yüksel[2,†] and Nils Paar[1,‡]
[1]Department of Physics, Faculty of Science, University of Zagreb, Bijenička c. 32, 10000 Zagreb, Croatia
[2]School of Mathematics and Physics, University of Surrey, Guildford, Surrey GU2 7XH, United Kingdom

(Received 16 January 2025; accepted 17 June 2025; published 2 July 2025)

- E1 → dominates the GDR region
- M1 → spin-flip resonance at lower energy

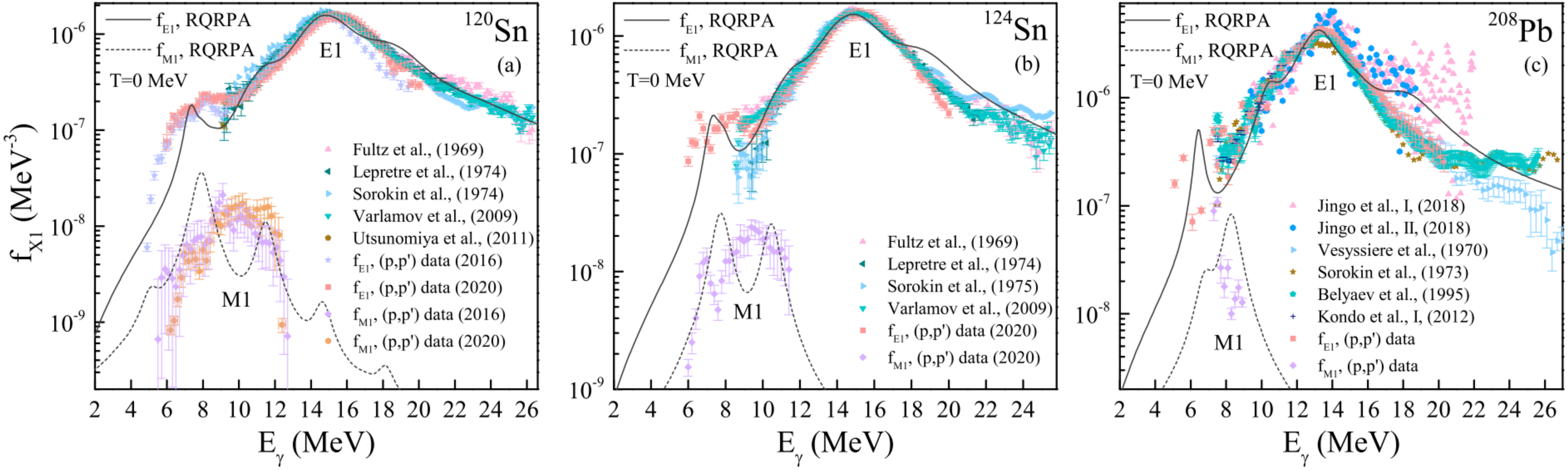

- At T=0, RQRPA reproduces the E1-dominated GDR region and the observed M1 spin-flip strength.
- This provides the baseline for finite-temperature E1+M1 γSF calculations.

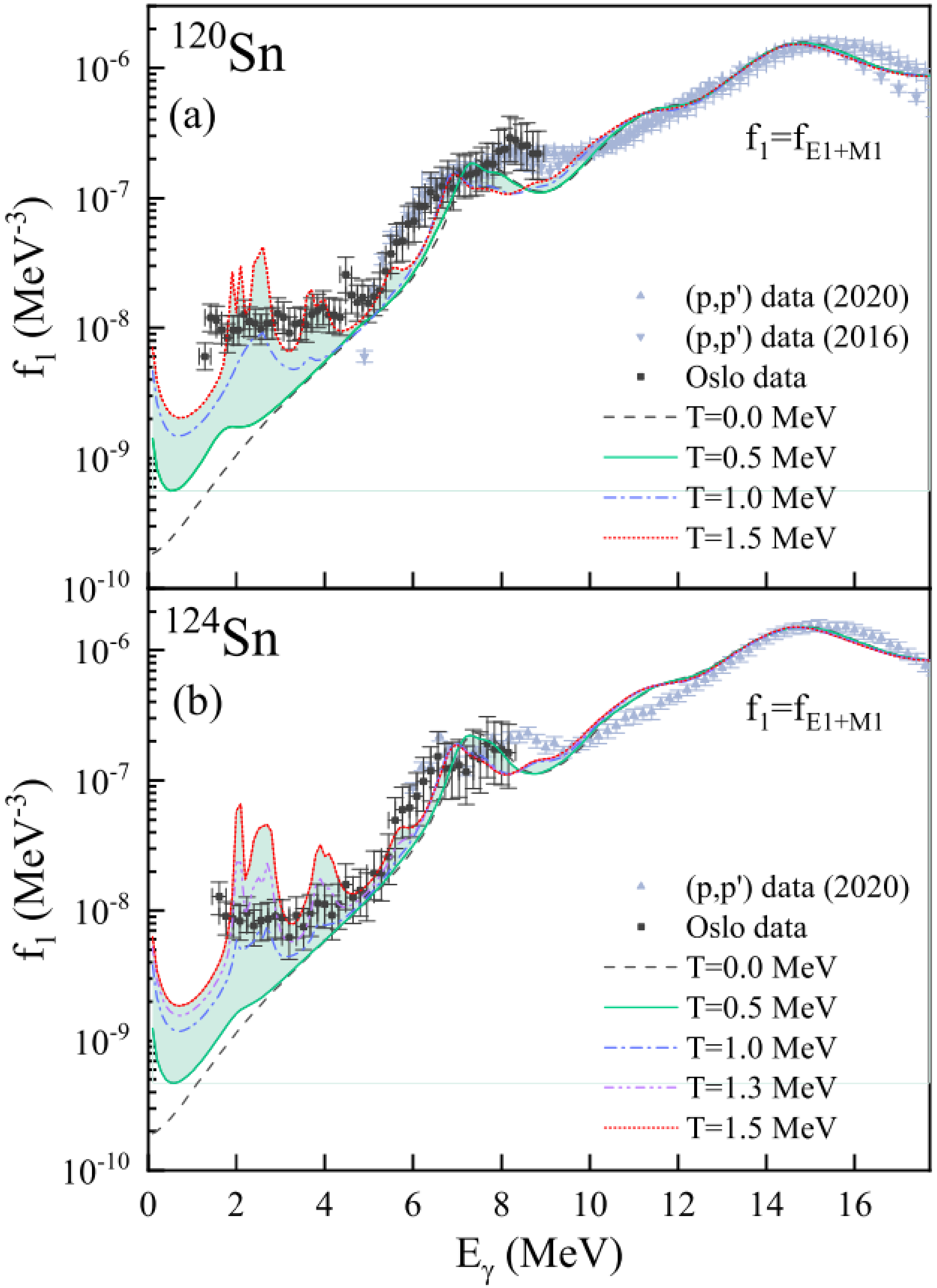

PHYSICAL REVIEW C **112**, 014307 (2025)

Electric and magnetic γ-ray strength functions at finite temperature

Amandeep Kaur[1,*] Esra Yüksel[2,†] and Nils Paar[1,‡]
[1]*Department of Physics, Faculty of Science, University of Zagreb, Bijenička c. 32, 10000 Zagreb, Croatia*
[2]*School of Mathematics and Physics, University of Surrey, Guildford, Surrey GU2 7XH, United Kingdom*

(Received 16 January 2025; accepted 17 June 2025; published 2 July 2025)

- FT-RQRPA $E1 + M1$ γSFs are calculated for $T = 0–1.5$MeV.
- The GDR region remains nearly unchanged with temperature, shows excellent agreement with the (p, p') data.
- The low-E_γ region is strongly enhanced by thermal effects, producing an upbend as $E_\gamma \to 0$.
- The $E_\gamma \approx 4–10$MeV region remains consistent with Oslo and (p, p')data.

PHYSICAL REVIEW C **112**, 014307 (2025)

Electric and magnetic γ-ray strength functions at finite temperature

Amandeep Kaur[1,*] Esra Yüksel[2,†] and Nils Paar[1,‡]
[1]Department of Physics, Faculty of Science, University of Zagreb, Bijenička c. 32, 10000 Zagreb, Croatia
[2]School of Mathematics and Physics, University of Surrey, Guildford, Surrey GU2 7XH, United Kingdom

(Received 16 January 2025; accepted 17 June 2025; published 2 July 2025)

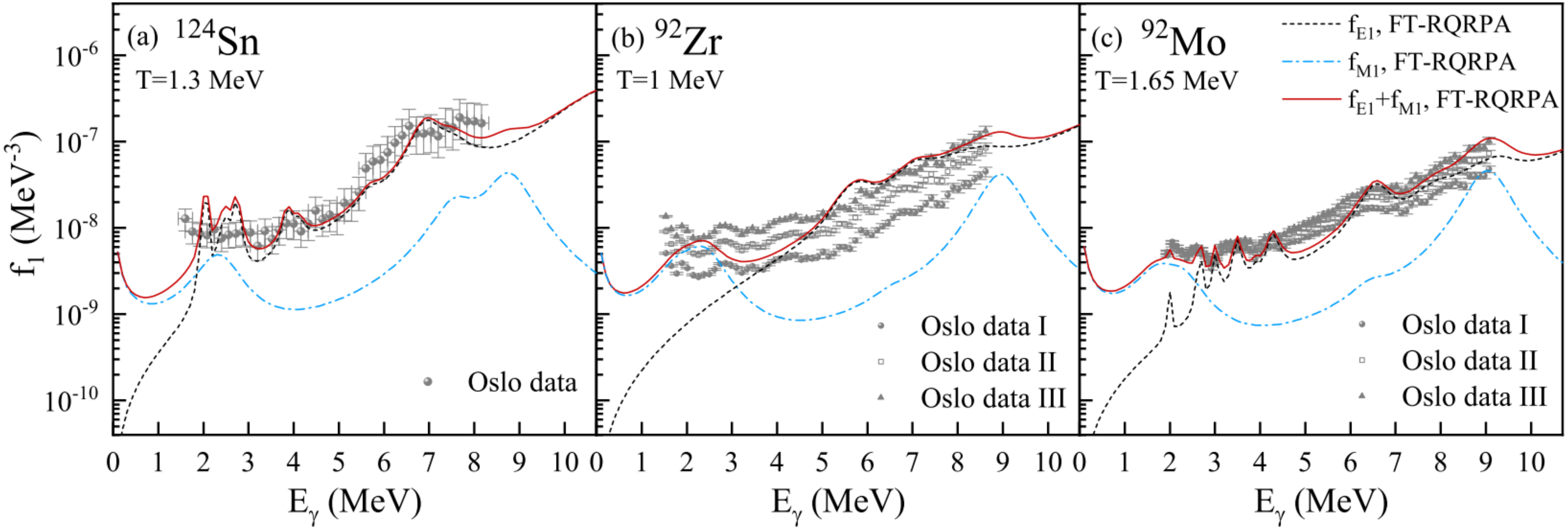

- Oslo data I, II and III represent the lower, recommended and upper limits of experimental measurements normalized within or at the limits of the range of uncertainties.

1. S. Goriely, et.al.,The European Physical Journal A 55, 172 (2019).
2. M. Guttormsen et.al., Phys. Rev. C 96, 024313 (2017).

Weak Transitions & Charge Exchange at finite temperature

- Charge-exchange excitations are nuclear excitations in which a neutron is converted into a proton, or a proton into a neutron, while the mass number A remains unchanged:

$$\text{Fermi (IAS):} \qquad \hat{F}_{\pm} = \sum_{i=1}^{A} \tau_{\pm}(i)$$

$$\text{Gamow–Teller (GT):} \qquad \hat{O}_{\mathrm{GT},\pm} = \sum_{i=1}^{A} \boldsymbol{\sigma}(i)\, \tau_{\pm}(i)$$

$$\text{Spin–dipole (SD):} \qquad \hat{O}_{\mathrm{SD},JM,\pm} = \sum_{i=1}^{A} r_i \left[Y_1(\hat{\mathbf{r}}_i) \otimes \boldsymbol{\sigma}(i) \right]_{JM} \tau_{\pm}(i)$$

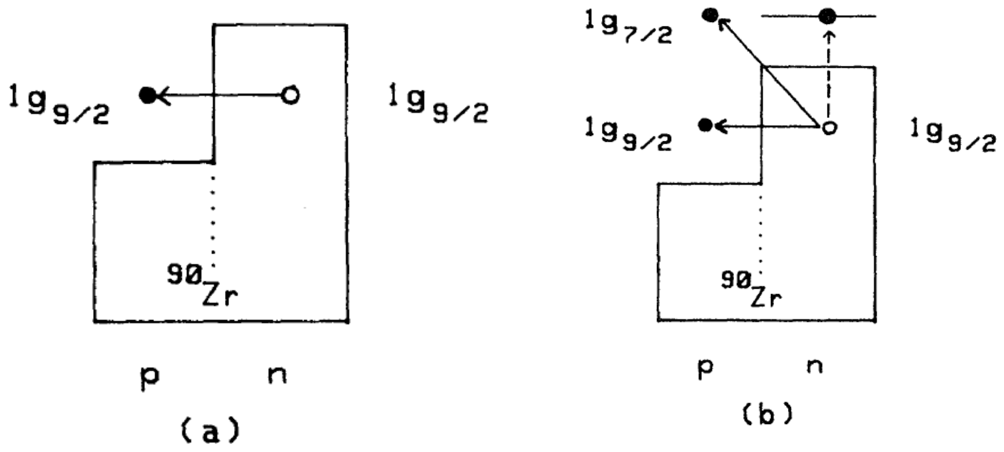

(a) the Fermi transition preserves the orbital, whereas (b) the Gamow–Teller transition also couples spin–orbit partner configurations *F. Osterfeld, Rev. Mod. Phys., 64, 491557 (1992)*.

- An accurate determination of spin–isospin excitations and related nuclear properties is essential for astrophysical calculations.

Isobaric analog states at finite temperature

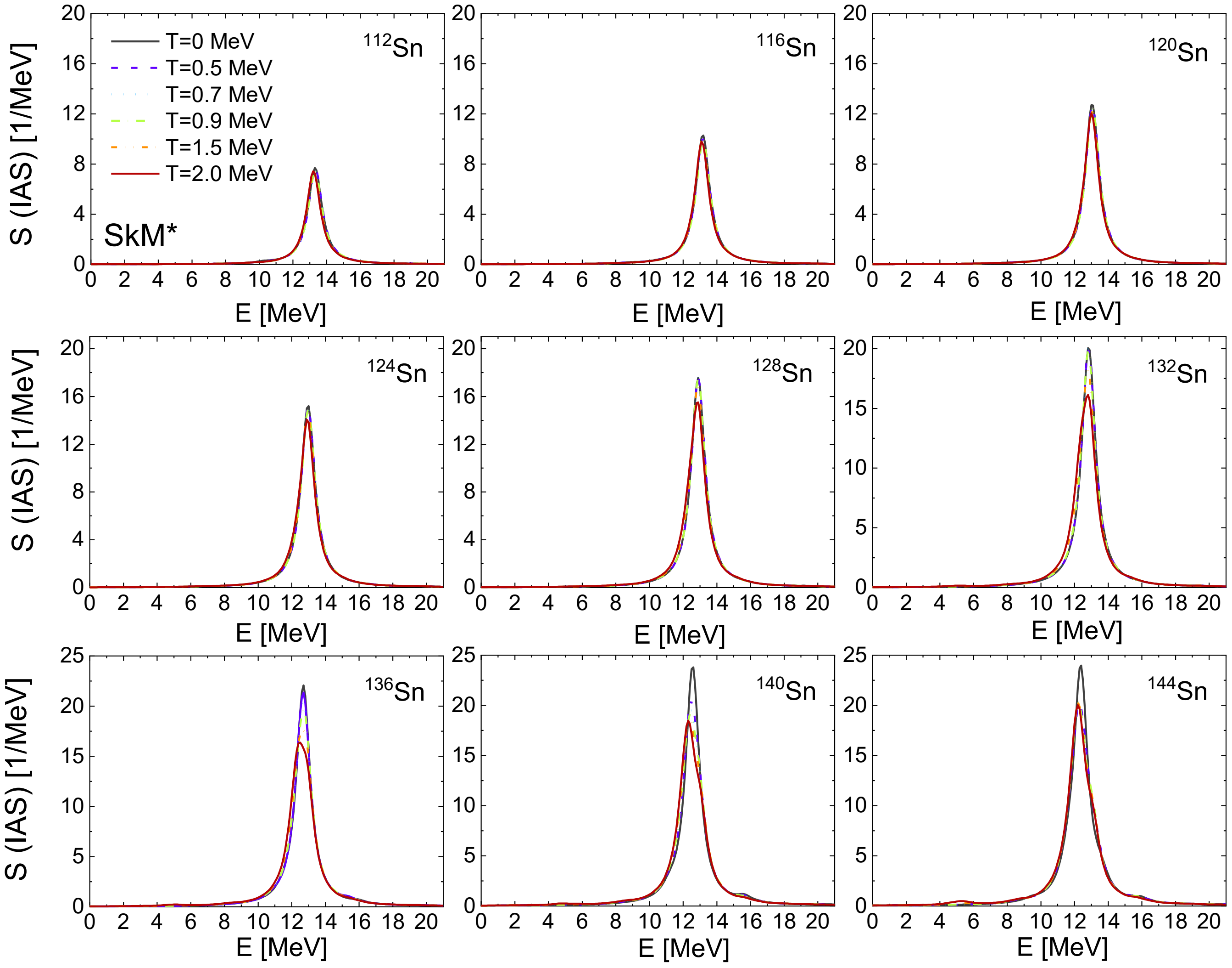

The IAS response in Sn nuclei with increasing temperature.

$$\hat{F}_{IAR} = \sum_{i=1}^{A} \tau_{-}(i)$$

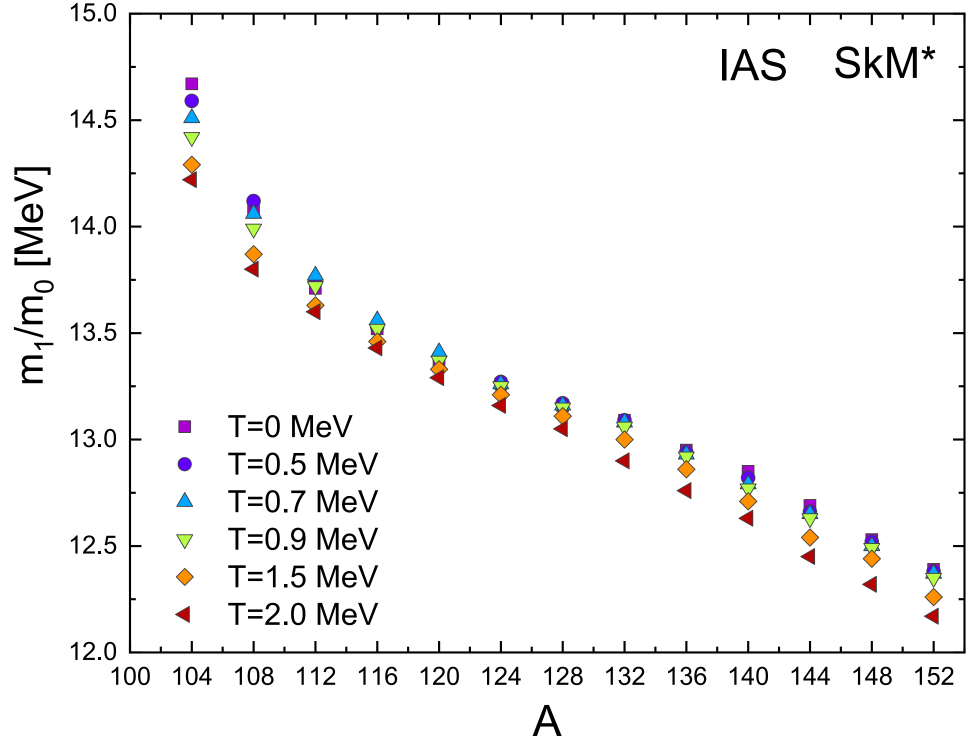

The centroid energy of the IAS in Sn nuclei with increasing temperature.

Spin dipole response at finite temperature

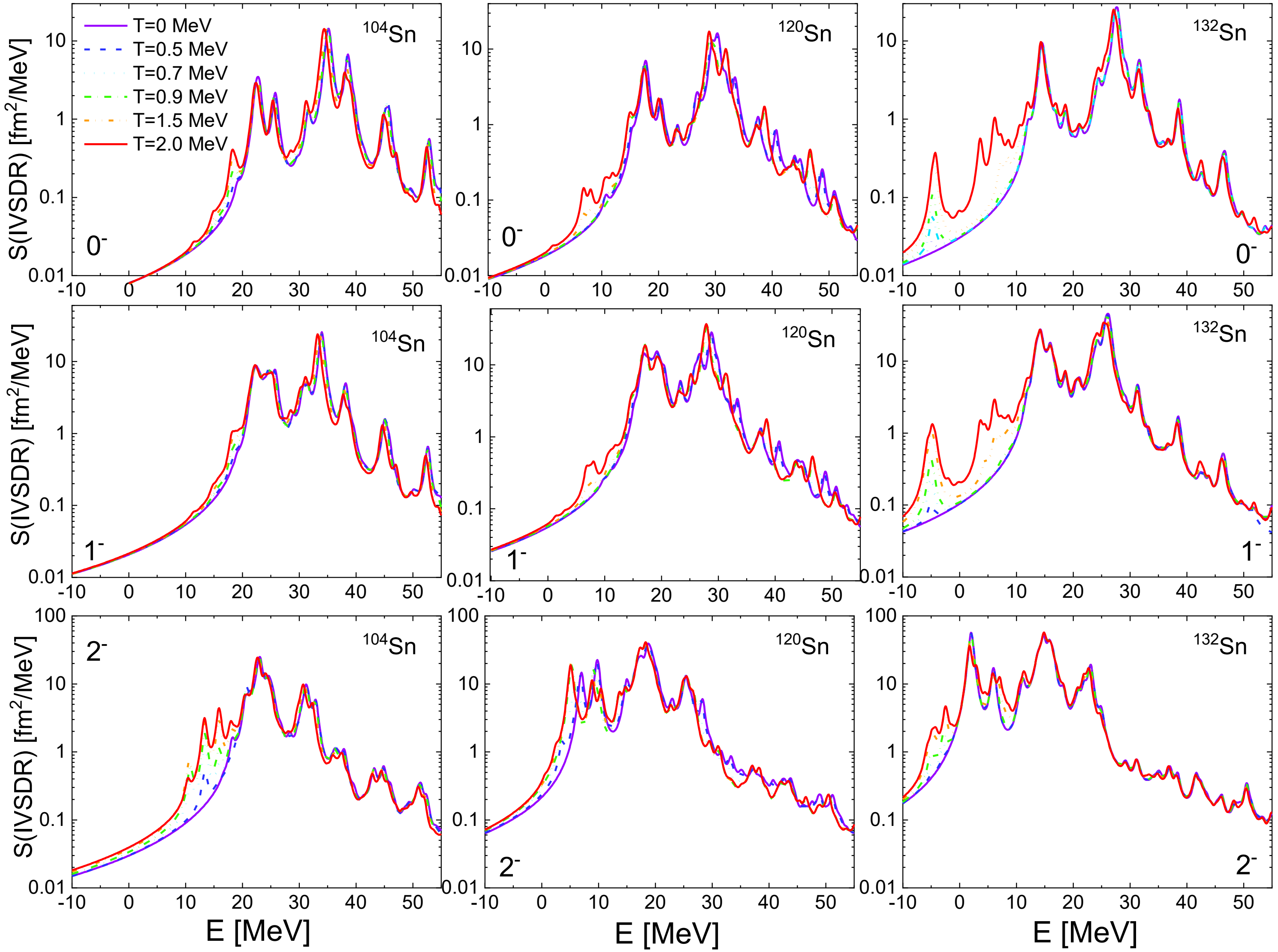

The spin-dipole resonance is excited by the operator

$$O_{IVSD\pm,J^\pi} = \sum_{i=1}^{A} r_i \left[\vec{Y}_1(\hat{r}_i) \otimes \vec{\sigma}(i)\right]_{J^\pi M} t_\pm(i),$$

$$\Delta L = 1;\ \Delta T = 1;\ \Delta S = 1;$$

It has three components $0^-;\ 1^-;\ 2^-$

- ✓ *Temperature has a considerable impact on the low-energy region of the excitation spectrum.*
- ✓ *Important for Beta-decay calculations*

Gamow-Teller states at finite temperature

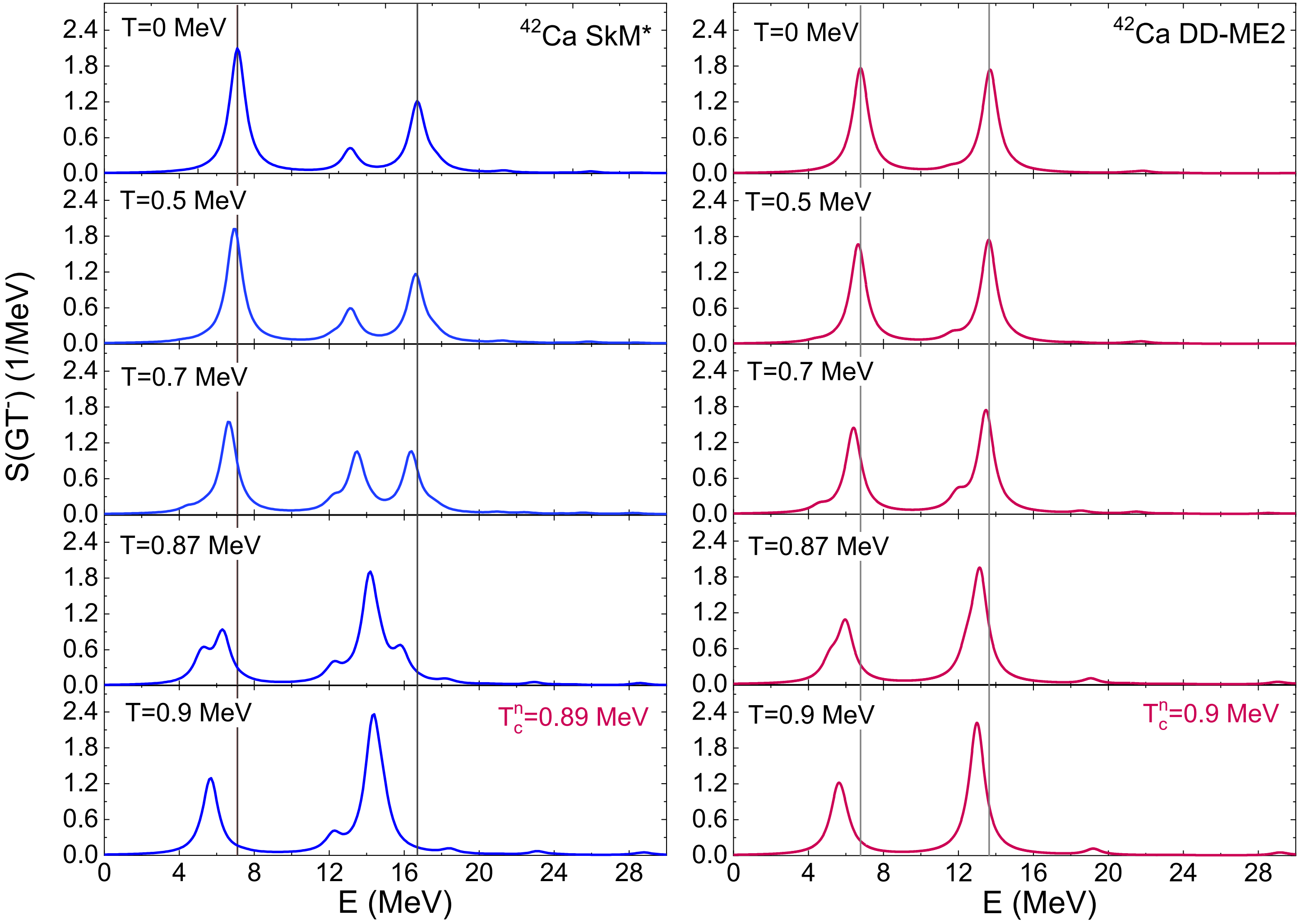

Gamow-Teller response at finite temperatures using relativistic and nonrelativistic functionals.

E. Yüksel, N. Paar, G. Colò, E. Khan, and Y. F. Niu, Phys. Rev. C 101, 044305, (2020).

Competition between pairing and temperature effects

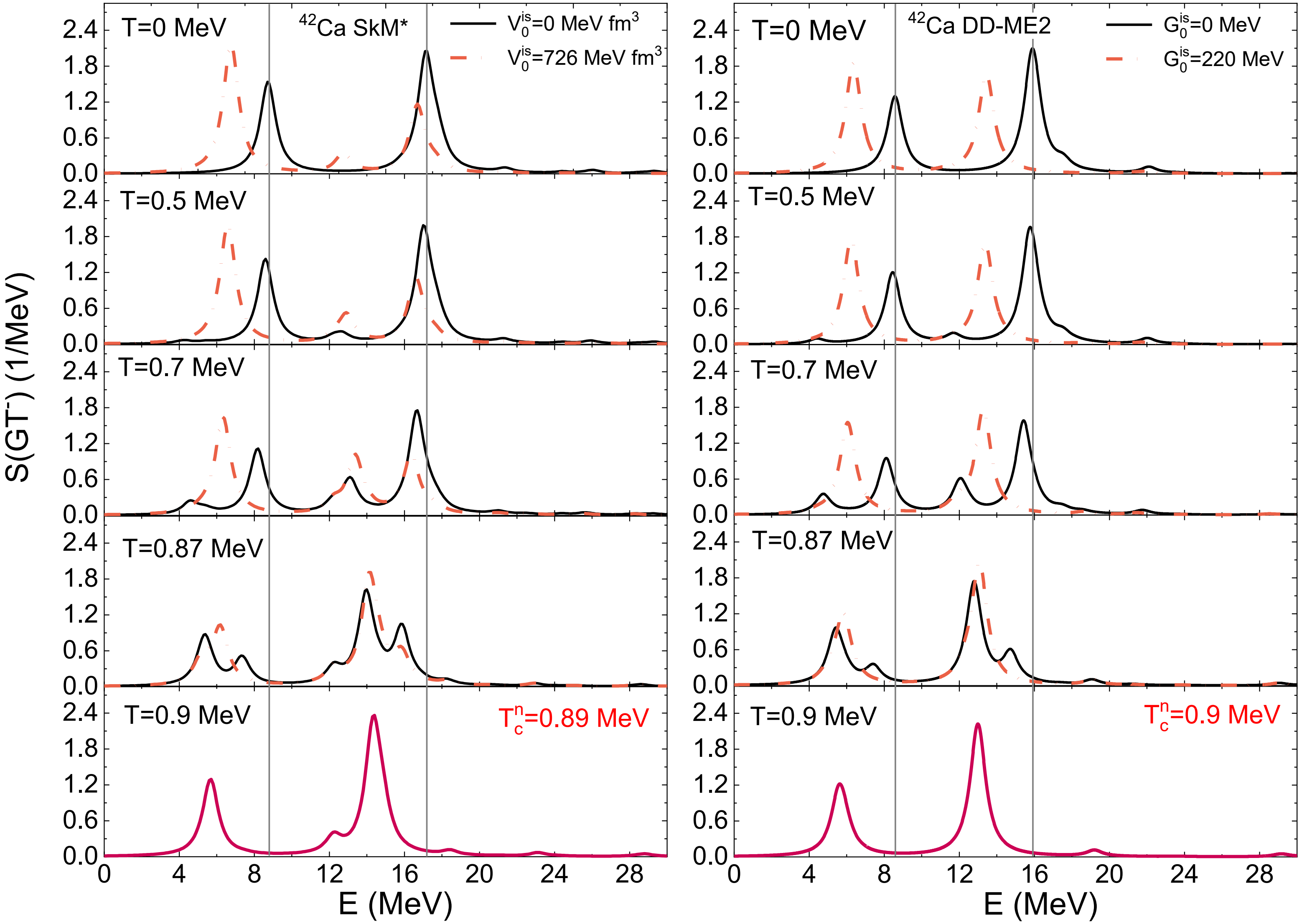

- *Without the isoscalar pairing,* the changes in the GT states are caused by the decrease of the isovector pairing effects and the softening of the repulsive ph interaction due to the temperature factors with increasing temperature.

1) $T \uparrow \Longrightarrow$ *IV pairing* $\downarrow \Longrightarrow E_{conf} \downarrow$
2) $T \uparrow \Longrightarrow V_{res} \downarrow \Longrightarrow E_x \downarrow$

- *With the inclusion of the isoscalar pairing,* the decrease in the excitation energies depends on the competition between the temperature and isoscalar pairing effects.

- *The temperature reduces the impact of the both isoscalar and the isovector pairing.*

***E. Yüksel**, N. Paar, G. Colò, E. Khan, and Y. F. Niu, Phys. Rev. C 101, 044305, (2020).*

Gamow-Teller states at finite temperature

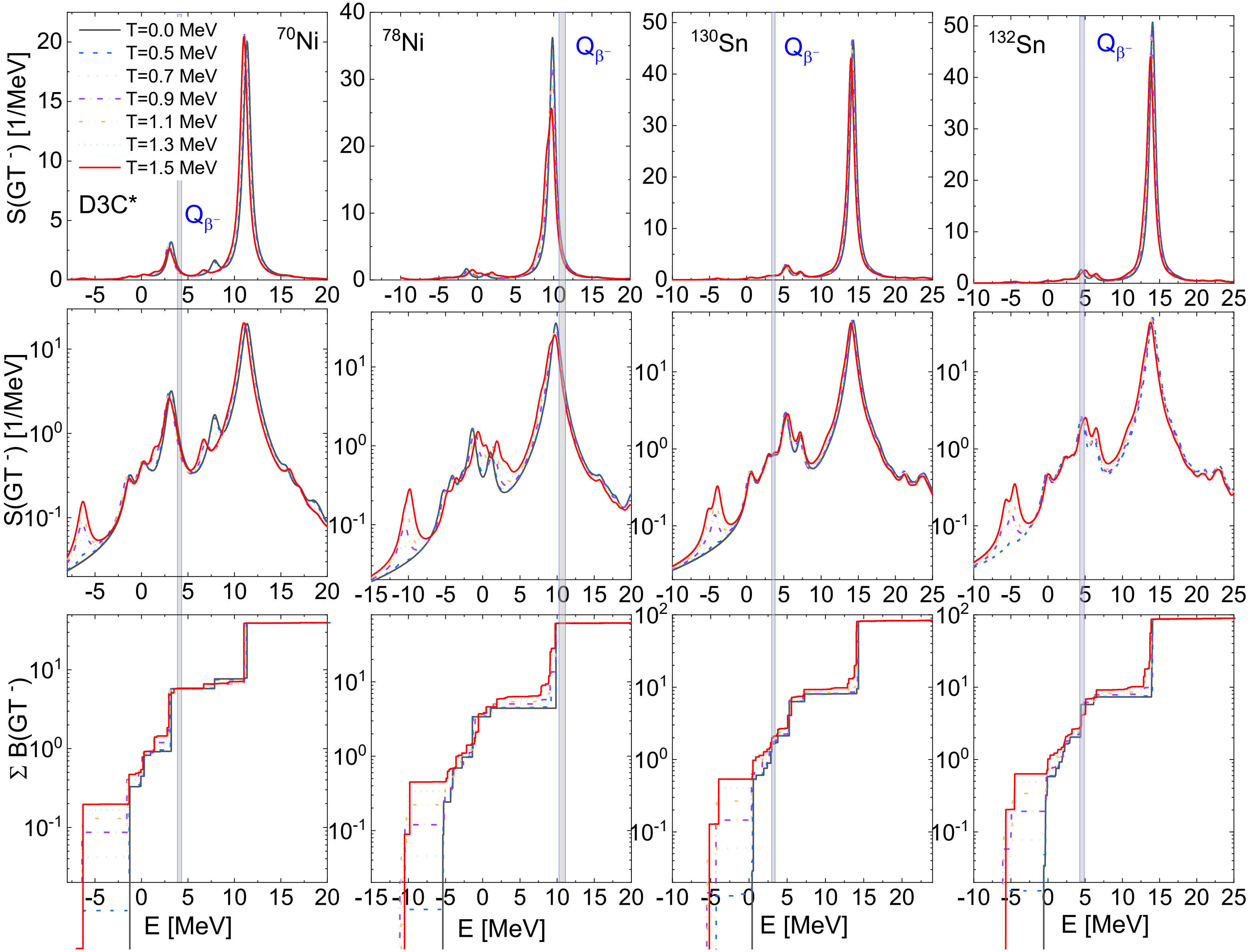

- ✓ *The new excitation channels become possible due to the smearing of the Fermi surface.*
- ✓ *The changes occur due to the temperature induced effects on the nuclear properties of nuclei and the residual particle-hole interaction.*
- ✓ Continuum plays an important role → transitions from thermally unblocked states give rise to an increase in the very low-energy region of the GT strength at finite temperatures.

Finite temperature relativistic time blocking approximation vs finite temperature RRPA.

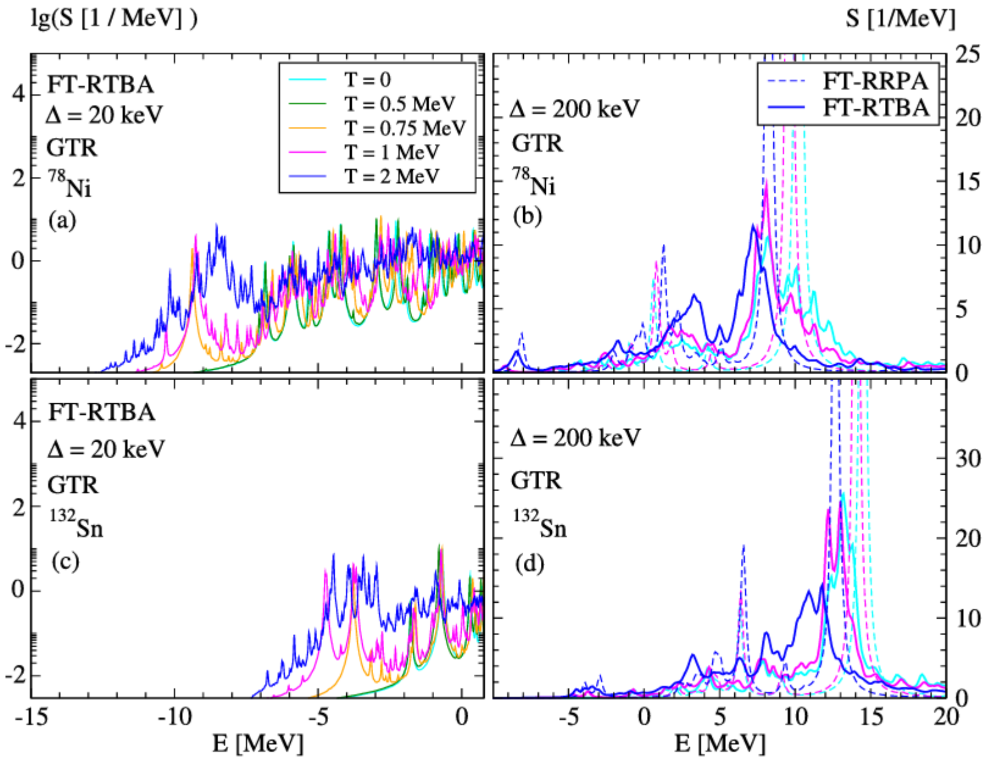

- Increasing temperature enhances and redistributes the GT− strength in 78Ni and 132Sn.

- The strength becomes more fragmented and spreads toward lower excitation energies, especially inside the Qβ window.

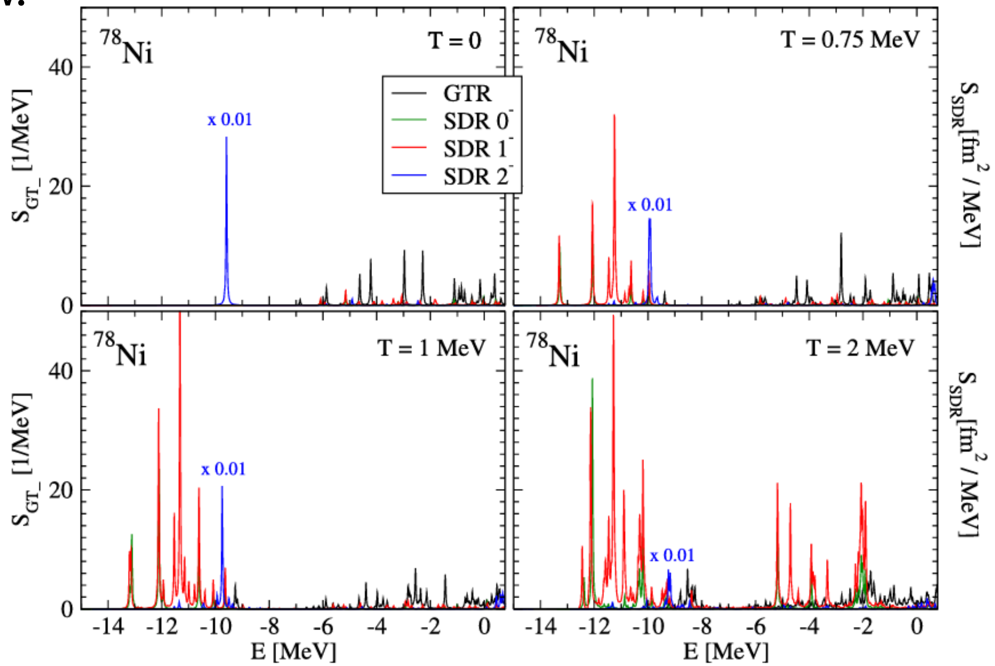

- Nuclei become more beta-unstable as temperature rises, with noticeable changes starting around T=0.5–0.75 MeV.

- This temperature dependence must be included when calculating beta-decay rates in hot astrophysical environments.

- The **first-forbidden spin-dipole transitions** also become increasingly important with temperature.

Beta-decay in stellar conditions

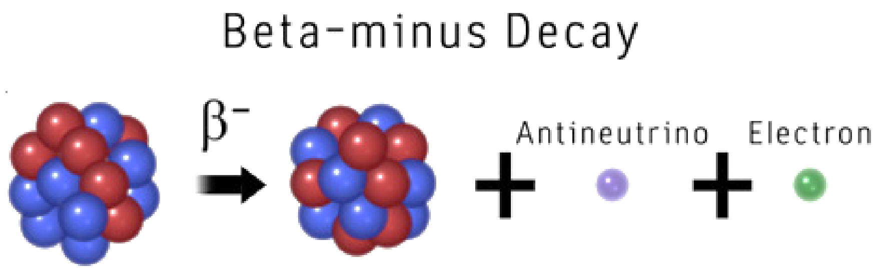

- ✓ Crucial for understanding stellar evolution and nucleosynthesis.
- ✓ Based on relativistic energy density functional theory and the proton-neutron Quasiparticle Random Phase Approximation

✓ The general form of β-decay rate in stellar conditions is

$$\lambda = \frac{\ln 2}{K} \int_0^{p_0} p_e^2 (W_0 - W)^2 F(Z, W) C(W) [1 - f(W)] d p_e$$

✓ For the allowed GT transitions, C(W) is equal to the reduced matrix element of the GT− transition

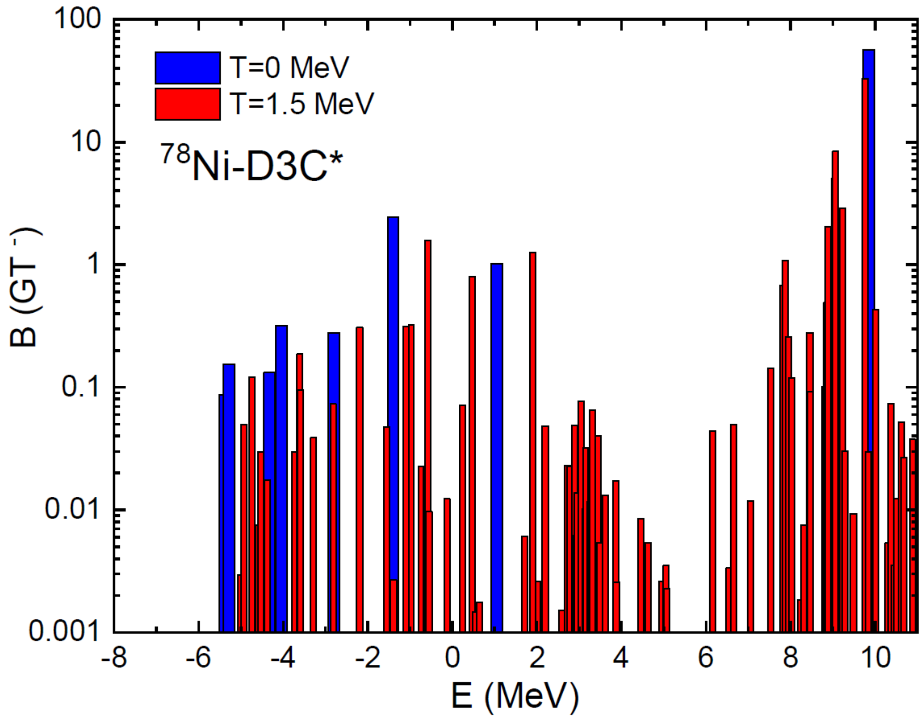

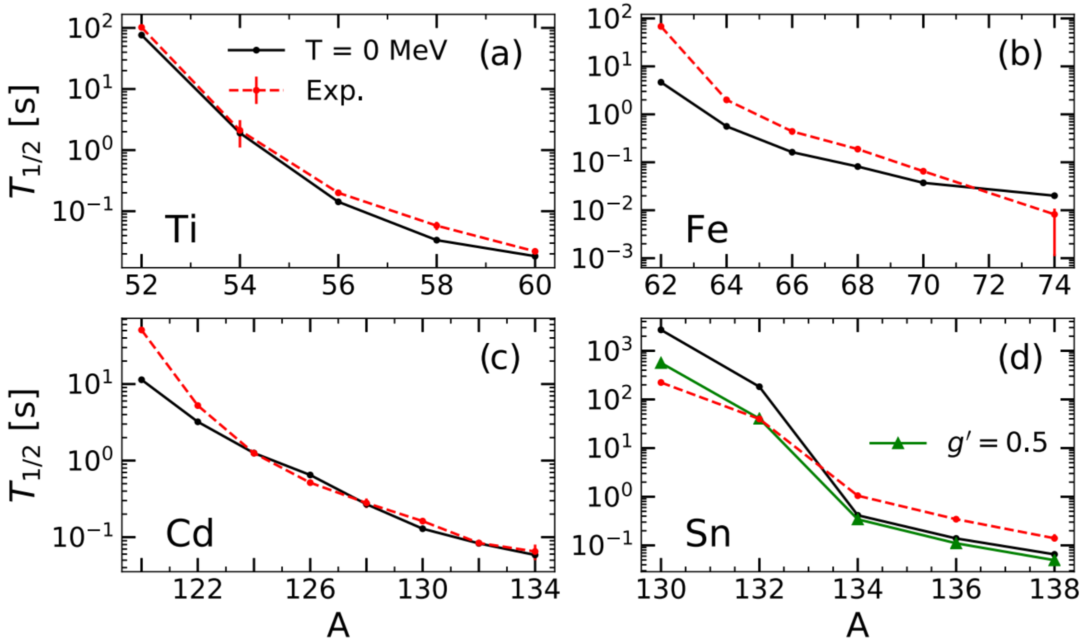

A. Ravlić, E. Yüksel, Y. F. Niu, N. Paar, PRC 104, 054318 (2021)

β-decay half-lives in stellar environments

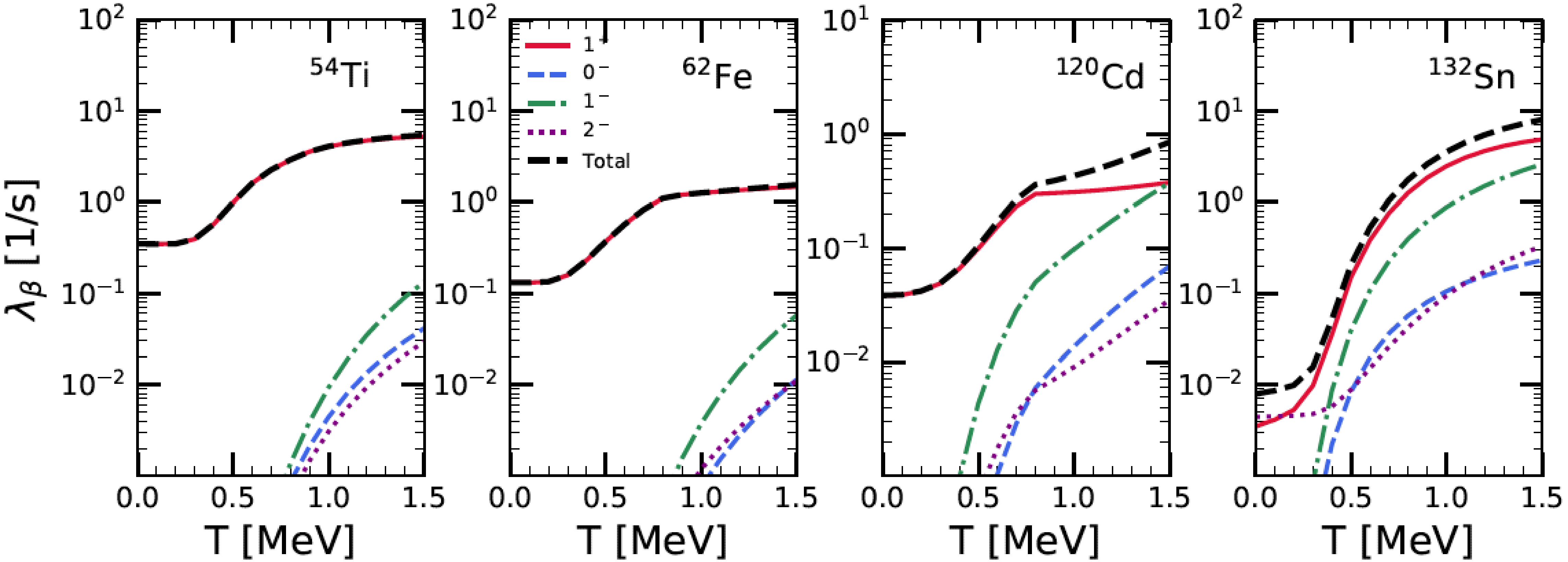

- Temperature dependence of β-decay rates λ_β for both allowed (1^+) and first-forbidden transitions ($0^-, 1^-, 2^-$) together with their total sum (Total) for ^{54}Ti, ^{62}Fe, ^{120}Cd, and ^{132}Sn. Calculations are performed at stellar density $\rho Ye = 10^7$ g/cm^3

A. Ravlić, E. Yüksel, Y. F. Niu, N. Paar, PRC 104, 054318 (2021)

β-decay half-lives in stellar environments

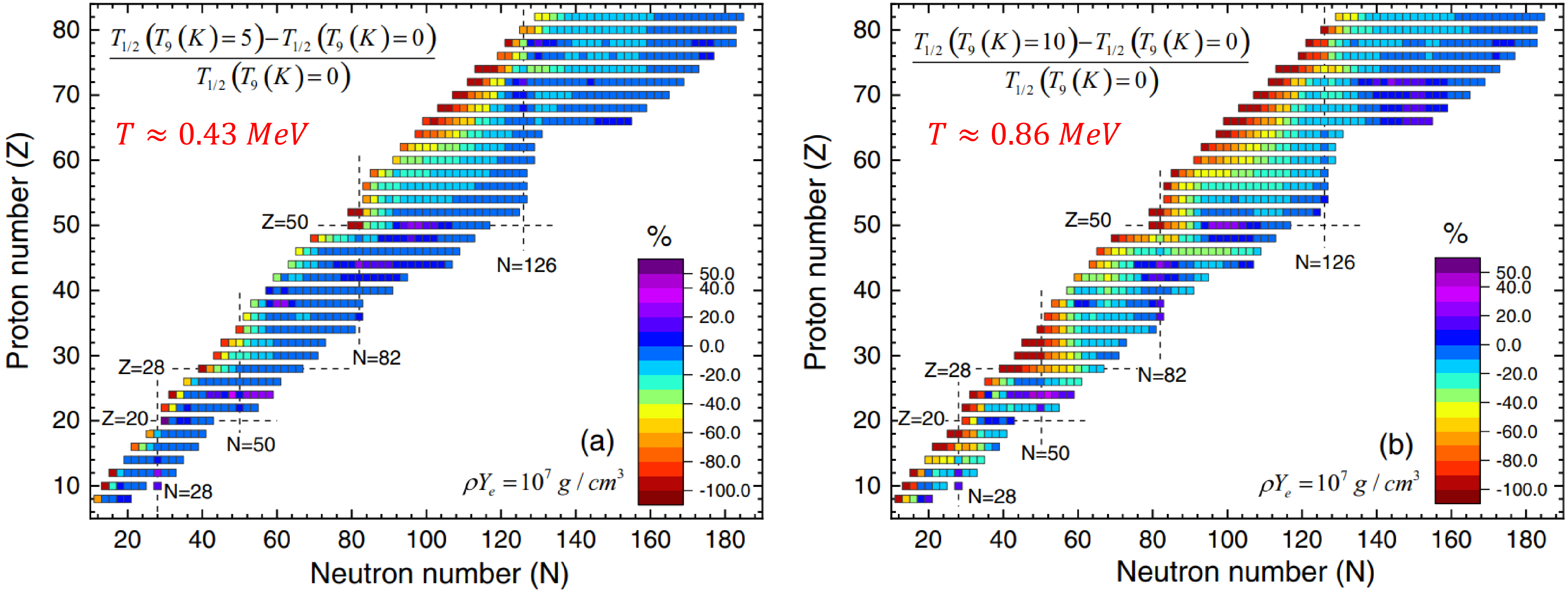

- In the majority of the nuclide map, a **decrease in the β-decay half-lives** is obtained **with increasing temperature**.
- Nuclei showing the most change are those with initially long half-lives (magic, semi-magic, and close to the valley of stability).

A. Ravlić, E. Yüksel, Y. F. Niu, N. Paar, PRC 104, 054318 (2021)

THANKS FOR LISTENING
Any questions?

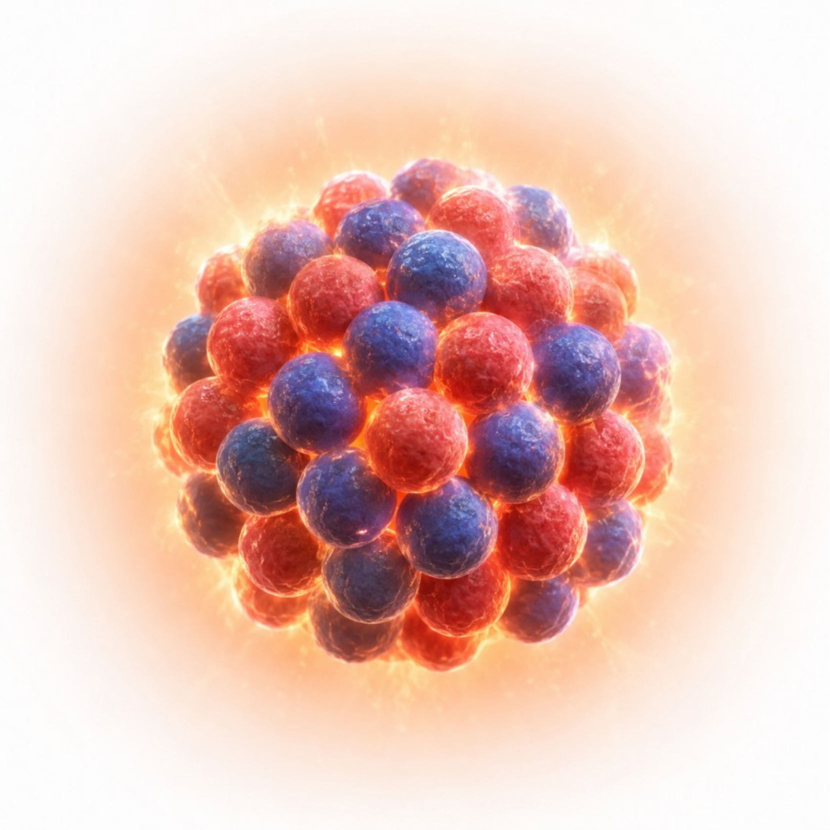

In Collaboration with:
Amandeep Kaur, Nils Paar, Ante Ravlic, , Gianluca Colo, Elias Khan, Yifei Niu, Kutsal Bozkurt.